Article

Cell Reports

NvPOU4/Brain3 Functions as a Terminal Selector Gene in the Nervous System of the Cnidarian *Nematostella vectensis*

Graphical Abstract

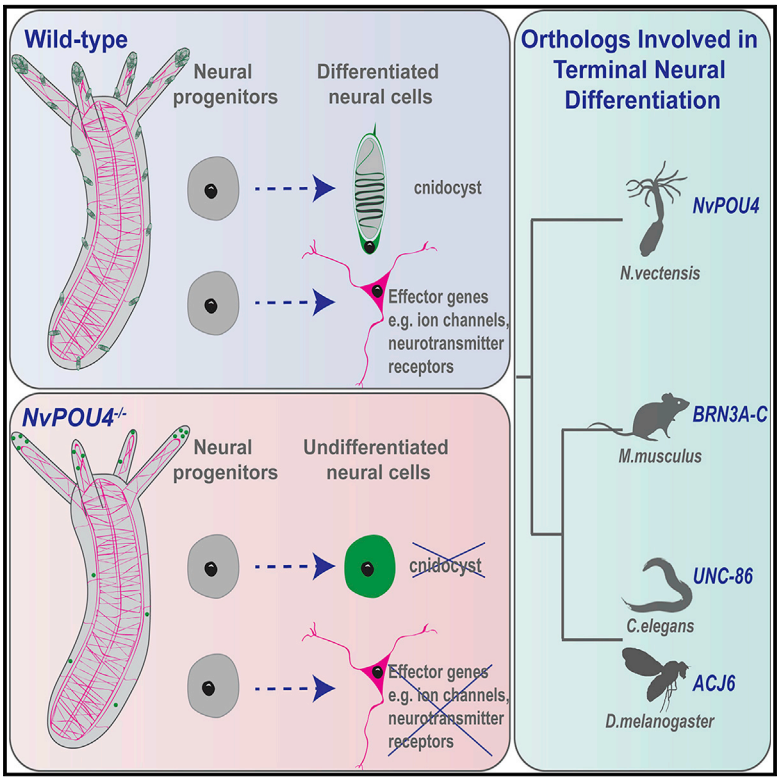

Highlights

- *NvPOU4* is broadly expressed in post-mitotic cells in the *Nematostella* nervous system
- Expression of *NvPOU4* is dependent on *NvSoxB(2)*
- Loss of *NvPOU4* affects the terminal differentiation of neurons and cnidocytes
- POU4 genes act as terminal selectors in evolutionarily distant animal clades

Authors

Océane Tournière, David Dolan, Gemma Sian Richards, Kartik Sunagar, Yaara Y. Columbus-Shenkar, Yehu Moran, Fabian Rentzsch

Correspondence

fabian.rentzsch@uib.no

In Brief

Using CRISPR mutants, transgenic lines, and cell-type-specific transcriptomes, Tournière et al. show that the transcription factor *NvPOU4* is required for the terminal differentiation of morphologically and molecularly disparate neural cells in the sea anemone *Nematostella vectensis*. These findings support an ancient role of POU4 genes as terminal selectors.

Tournière et al., 2020, Cell Reports *30*, 4473–4489
March 31, 2020
https://doi.org/10.1016/j.celrep.2020.03.031

CellPress

Cell Reports
Article

NvPOU4/Brain3 Functions as a Terminal Selector Gene in the Nervous System of the Cnidarian *Nematostella vectensis*

Océane Tournière,[1] David Dolan,[2] Gemma Sian Richards,[1] Kartik Sunagar,[3,4] Yaara Y. Columbus-Shenkar,[3] Yehu Moran,[3] and Fabian Rentzsch[1,5,6,*]

[1]Sars International Centre for Marine Molecular Biology, University of Bergen, 5006 Bergen, Norway
[2]Computational Biology Unit, Department for Informatics, University of Bergen, 5006 Bergen, Norway
[3]Department of Ecology, Evolution and Behaviour, Alexander Silberman Institute of Life Sciences, The Hebrew University of Jerusalem, 9190401 Jerusalem, Israel
[4]Evolutionary Venomics Lab, Centre for Ecological Sciences, Indian Institute of Science, Bangalore 560012, India
[5]Department for Biological Sciences, University of Bergen, 5006 Bergen, Norway
[6]Lead Contact
*Correspondence: fabian.rentzsch@uib.no
https://doi.org/10.1016/j.celrep.2020.03.031

SUMMARY

Terminal selectors are transcription factors that control the morphological, physiological, and molecular features that characterize distinct cell types. Here, we show that, in the sea anemone *Nematostella vectensis, NvPOU4* is expressed in post-mitotic cells that give rise to a diverse set of neural cell types, including cnidocytes and *NvElav1*-expressing neurons. Morphological analyses of *NvPOU4* mutants crossed to transgenic reporter lines show that the loss of *NvPOU4* does not affect the initial specification of neural cells. Transcriptomes derived from the mutants and from different neural cell populations reveal that *NvPOU4* is required for the execution of the terminal differentiation program of these neural cells. These findings suggest that POU4 genes have ancient functions as terminal selectors for morphologically and functionally disparate types of neurons and they provide experimental support for the relevance of terminal selectors for understanding the evolution of cell types.

INTRODUCTION

Neurons display a remarkable morphological and molecular diversity. The acquisition of the features that characterize different types of neurons is the result of a series of developmental processes largely directed by transcription factors and signaling molecules (Edlund and Jessell, 1999). Early stages of neural development are often characterized by the proliferation of different types of progenitor cells via symmetric and/or asymmetric divisions (Doe, 2008; Homem et al., 2015; Taverna et al., 2014). After their terminal mitosis, the differentiation of neurons typically begins with the occurrence of more general neural features, like the expression of neural cytoskeletal proteins and by the formation of neurites (Ernsberger, 2012; Stefanakis et al., 2015). The terminal identity of individual types of neurons eventually manifests by the expression of specific neurotransmitter systems, the elaboration of specific projection patterns, and other factors defining the physiological properties of these neuron types. Transcription factors that regulate these terminal differentiation features of distinct neuron types are called terminal selector genes (Allan and Thor, 2015; Hobert, 2016; Hobert and Kratsios, 2019). Terminal selectors often function in combination and may affect all or only some aspects of the identity of a neuron (e.g., Etchberger et al., 2007; Stratmann et al., 2019). Although transcription factors regulating the terminal differentiation of neurons have been identified in several bilaterians (Allan and Thor, 2015; Hobert and Kratsios, 2019), it is currently unknown whether conserved terminal selectors tend to have comparable functions over long evolutionary distances. We address this question here by analyzing the function of the Pit/Oct1/UNC-86 (POU) domain transcription factor *POU4/Brn3* in a representative of a non-bilaterian animal clade, the cnidarian *Nematostella vectensis*.

Cnidarians are the sister group of bilaterians (Dunn et al., 2014; Telford et al., 2015), with the separation of these two lineages estimated to have occurred over 600 mya (dos Reis et al., 2015; Park et al., 2012). As adults, they possess a relatively simple nervous system that lacks brain-like centralization. Their nervous system comprises three main classes of neural cells: cnidocytes (“stinging cells,” cnidarian-specific mechano/chemoreceptor cells); ganglion cells (interneuron-like cells); and sensory/sensory-motor cells (Galliot et al., 2009; Rentzsch et al., 2019; Watanabe et al., 2009). Morphological and molecular analyses suggest the existence of distinct subpopulations of these classes of neural cells; however, an integrated characterization of neural cell types in cnidarians is currently lacking (Rentzsch et al., 2019; Sebé-Pedrós et al., 2018; Siebert et al., 2019). The sea anemone *Nematostella vectensis* belongs to the anthozoan class of cnidarians. Due to its inducible fertilization, its relatively short generation time, and amenability to molecular manipulations, *Nematostella* has become an important cnidarian model organism (Layden et al., 2016). It has previously been shown that a large fraction of its neurons derives from a pool of *NvSoxB(2)*-expressing neural progenitor cells (NPCs) located

in both ectoderm and endoderm, which give rise to the three classes of neural cells (Nakanishi et al., 2012; Richards and Rentzsch, 2014). In addition to *NvSoxB(2)*, the basic helix-loop-helix (bHLH) genes *NvAshA* and *NvAtonal-like* have been identified as positive regulators of neurogenesis, whereas Notch signaling acts to restrict the number of neural progenitor cells (Layden et al., 2012; Layden and Martindale, 2014; Rentzsch et al., 2017; Richards and Rentzsch, 2015). For the regulation of early stages of neuron development, these observations suggest a considerable degree of conservation between *Nematostella* and bilaterians. How the terminal differentiation of neurons is regulated in *Nematostella* is currently poorly understood. Accordingly, it is not known whether the conservation of neurogenic transcriptional programs between *Nematostella* and bilaterians extends to the late stages of neuron development.

POU genes are transcription factors that contain a bipartite DNA binding domain consisting of a POU-specific and a homeobox domain. Although being found only in metazoans, they diversified early during animal evolution, and four classes of POU genes were present in the last common ancestor of all living animals (Gold et al., 2014; Larroux et al., 2008). Genes of the POU4 class are predominantly expressed in neuronal cells and have been shown to regulate the terminal differentiation of these neurons in several organisms. In mammals, there are three POU4 genes, *Brn3a*, *Brn3b*, and *Brn3c*, all of which are prominently expressed in partially overlapping areas of sensory structures, as well as in other parts of the nervous system (Collum et al., 1992; Fedtsova and Turner, 1995; Gerrero et al., 1993; Ninkina et al., 1993; Turner et al., 1994; Xiang et al., 1993, 1995). Analyses of knockout mice have identified key roles for these genes in the formation of hair cells in the auditory and vestibular systems (*Brn3c*; Erkman et al., 1996; Xiang et al., 1997), of retinal ganglion cells (*Brn3b*; Erkman et al., 1996; Gan et al., 1996), and of somatosensory and brainstem neurons (*Brn3a*; McEvilly et al., 1996; Xiang et al., 1996). Each of the Brn3 genes functions mainly at later stages of neural differentiation, e.g., in the acquisition of morphological features of somatosensory neurons and retinal ganglion cells (Badea et al., 2009, 2012; Erkman et al., 2000; Ryan and Rosenfeld, 1997). In *Drosophila*, the POU4 ortholog *acj6*/*I-POU* regulates synaptic targeting in the central nervous system and the odor sensitivity of olfactory neurons (Ayer and Carlson, 1991; Certel et al., 2000; Clyne et al., 1999; Treacy et al., 1992). In the nematode *Caenorhabditis elegans*, the single POU4 gene, *unc-86*, is expressed in several types of neurons (Finney and Ruvkun, 1990). In most of these neurons, *unc-86* acts in specific combinations with other transcription factors to control a terminal differentiation program, for example, by defining the neurotransmitter identity of the cell (Chalfie et al., 1981; Duggan et al., 1998; Hobert, 2016; Serrano-Saiz et al., 2013; Zhang et al., 2014). This terminal selector function of POU4 genes is often also required for the maintenance of the identity of these neurons, both in *C. elegans* and in mice (Serrano-Saiz et al., 2018). In addition to its role in terminal differentiation, *unc-86* has a role in regulating the division of some neural progenitor cells (Chalfie et al., 1981; Finney and Ruvkun, 1990). In line with potential roles in the nervous system, POU4 genes are expressed in sensory and other neural structures in several other bilaterians (Backfisch et al., 2013; Candiani et al., 2005, 2006; Nomaksteinsky et al., 2013; O'Brien and Degnan, 2002; Ramachandra et al., 2002; Wollesen et al., 2014). Overall, their roles in different types of neurons and in several bilaterians make POU4 genes prime candidates for addressing the early evolution of terminal neural differentiation.

Outside bilaterians, little is known about the role of POU4 genes. In medusae of the cnidarians *Aurelia sp*. and *Craspedacusta sowerbyi*, *POU4* expression was detected in sensory structures at the margin of the bell (Hroudova et al., 2012; Nakanishi et al., 2010); however, no functional analyses have been reported so far in these groups. In this study, we use gene expression analyses and an *NvPOU4*::memGFP transgenic reporter line to show that the single *Nematostella* POU class 4 gene is expressed in a large and heterogeneous population of post-mitotic neural cells. Furthermore, we generated an *NvPOU4* mutant line by CRISPR/Cas9-mediated genome editing, analyzed the transcriptome of the mutants, and crossed it to nervous-system-specific transgenic reporter lines. This revealed that *NvPOU4* functions in the terminal differentiation of neural cells, including the cnidarian-specific cnidocytes. These observations indicate that POU4 genes have ancient roles in terminal neural differentiation and that the regulation of cell differentiation by terminal selector genes evolved early in animal evolution.

RESULTS

NvPOU4 Is Expressed in Neural Cells from Early Blastula to Polyp Stage

The *Nematostella* genome contains a single POU4 gene (Putnam et al., 2007; Larroux et al., 2008; Gold et al., 2014). Using whole-mount *in situ* hybridization, we first observed expression of *NvPOU4* in few cells at early blastula (12 h post fertilization at 21°C; Figure 1A). This expression occurs after the start of *NvSoxB(2)* expression (a gene expressed in neural progenitor cells; Magie et al., 2005; Richards and Rentzsch, 2014) but before expression of *NvNCol3* commences (a gene expressed in differentiating cnidocytes and encoding the minicollagen structural protein of the cnidocyst capsule wall; Babonis and Martindale, 2017; Zenkert et al., 2011). *NvPOU4* is expressed in scattered cells all over the ectoderm of the embryo at gastrula stage and in scattered single cells in both ectoderm and endoderm at mid-planula stage (Figures 1B and 1C). At late planula stage, the expression is prominent in cells close to the oral opening (Figure 1D). At tentacle bud stage, this expression has resolved into four distinct patches, the developing tentacle buds (Figure 1E). In primary polyps, expression of *NvPOU4* is still detectable in scattered ectodermal and endodermal cells and, most prominently, in the tentacle tips (Figure 1F). The expression in scattered cells throughout the body column resembles that of several neural genes described previously (Layden et al., 2012; Marlow et al., 2009; Nakanishi et al., 2012), whereas the expression in the tentacle buds and tentacle tips reflects the main sites of cnidocyte formation (Babonis and Martindale, 2017; Zenkert et al., 2011).

NvPOU4 starts being expressed approximately 2 h after the expression of *NvSoxB(2)* (Figure S1), a gene that is broadly required for neurogenesis in *Nematostella* (Richards and Rentzsch, 2014). To understand better whether *NvPOU4* is

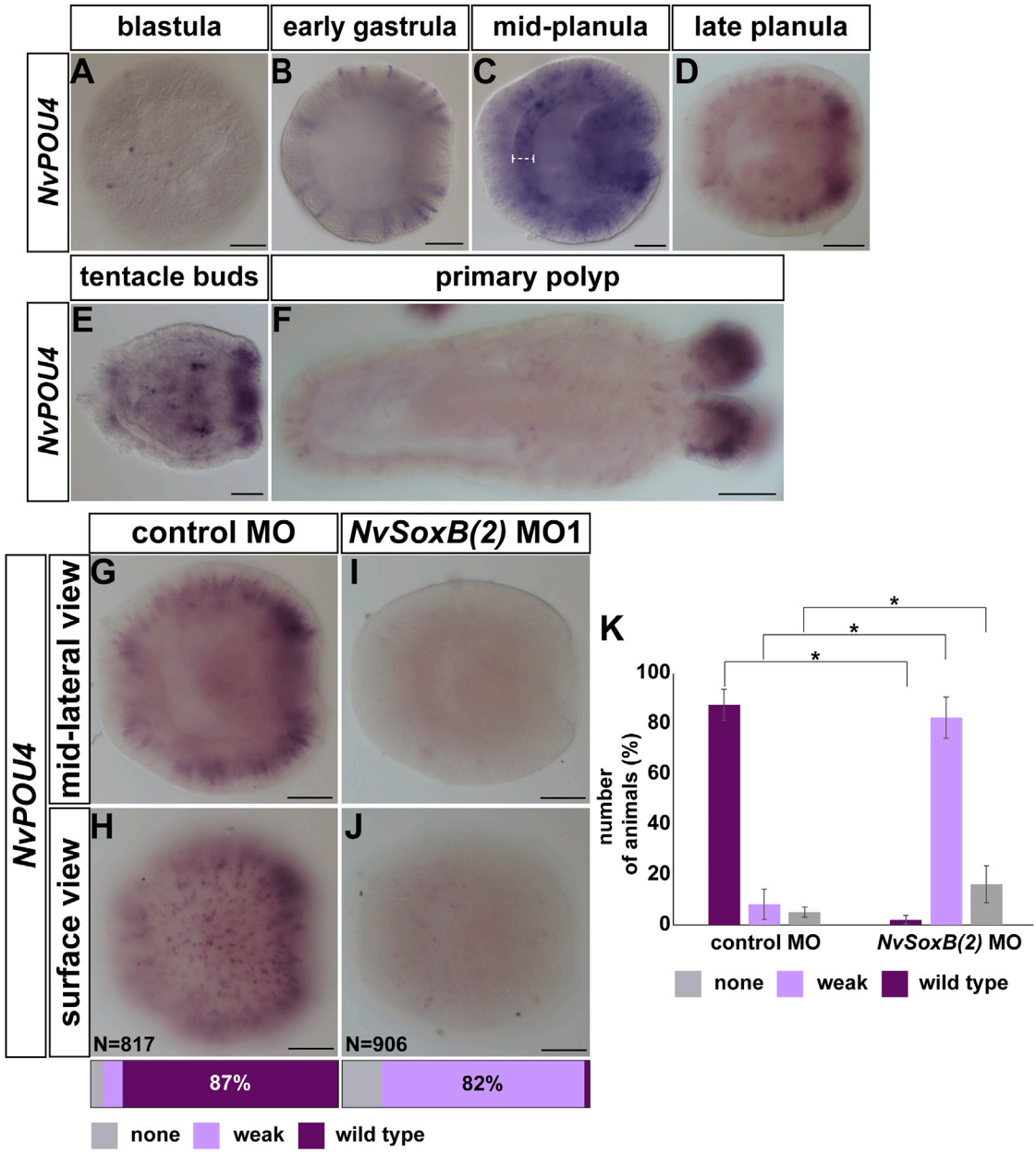

Figure 1. *NvPOU4* Expression Is Controlled by *NvSoxB(2)*

(A–F) *In situ* hybridization with probes indicated on the left side and the developmental stage on top. Mid-lateral views with the aboral pole to the left are shown. The white bracket in (C) indicates the endoderm layer. *NvPOU4* is expressed in scattered single cells all over the embryos. All *in situ* hybridizations were done on at least three biological replicates with n > 20 for each sample.

(G–J) *In situ* hybridization with *NvPOU4* probe. Treatments are indicated to the top of each image; *NvSoxB(2)* morpholino (MO) condition is compared to control MO-injected animals. (G and H) and (I and J) are different focal planes of the same specimens. *NvSoxB(2)* MO injection results in a decreased number of *NvPOU4*-expressing cells. Animals were quantified into phenotypic classes based on having no, weak, or wild type expression. (I) and (J) are examples of weak expression. Bars at the base of each image represent the percentage of animals in each phenotypic class.

(K) Graphical representation of the percentage of animals in each phenotypic class shown as mean ± SD (four biological replicates). Significance was tested by chi-square test for control MO versus *NvSoxB(2)* MO for the different categories (WT, weak, none) using the count data. For "WT" and for "weak," $p < 2.2 \times 10^{-6}$; for "none," $p = 0.0002948$. Asterisks indicate significance at $p < 0.001$.

Scale bars represent 50 μm.

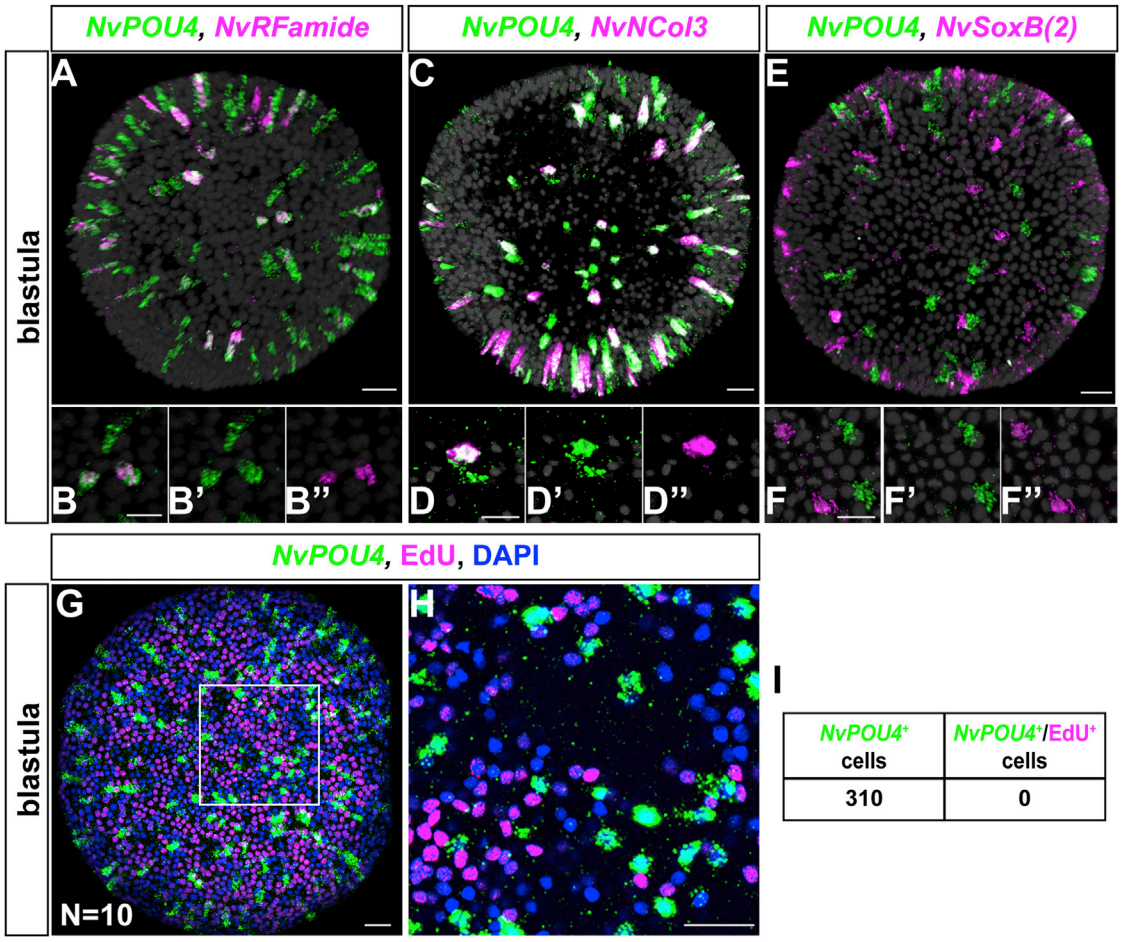

Figure 2. *NvPOU4* Is Expressed in Differentiating Cells

(A–F) Double fluorescence *in situ* hybridization at blastula stage for *NvPOU4* (green) and either *NvRFamide*, *NvNcol3*, or *NvSoxB(2)* (magenta). DAPI is shown in gray. The neural differentiating markers *NvRFamide* (A and B) and *NvNCol3* (C and D) show partial co-expression (white) with *NvPOU4*. No co-expression with the NPC marker *NvSoxB(2)* was detected (E and F). (A), (C), and (E) are projections of stacks; all other images are single confocal sections. Stacks are available as Videos S1, S2, and S3. White color in (E) is caused by the maximal projection and does not represent co-labeling of *NvPOU4* and *NvSoxB(2)*. For gastrula and planula stages, see Figure S2 and Videos S4–S9. All *in situ* hybridizations were performed with at least three replicates.

(G and H) Fluorescence *in situ* hybridization for *NvPOU4* (green) plus staining for EdU (magenta) and DAPI (blue) at blastula stage. (G) is a projection of a stack, and (H) is a single confocal section. The white rectangle in (G) indicates the area shown in (H). The stack for (G) is available as Video S10.

(I) In a 100 μm × 100 μm area of mid-lateral ectoderm of 310 *NvPOU4*-expressing cells (in 10 animals), none incorporated EdU, suggesting that *NvPOU4*-expressing cells are post-mitotic.

All *in situ* hybridizations and the EdU labeling were performed with at least three biological replicates, i.e., animals derived from three different spawnings. Scale bars represent 20 μm.

expressed in cells of the neural lineage, we inhibited the function of *NvSoxB(2)* by injection of a morpholino antisense oligonucleotide (Richards and Rentzsch, 2014). This resulted in a nearly complete suppression of *NvPOU4* expression (Figures 1G–1K).

Taken together, the expression pattern and the dependence on *NvSoxB(2)* suggest that *NvPOU4* is expressed in neural cells in *Nematostella*.

NvPOU4 Expression Is Restricted to Non-proliferating, Differentiating Cells

To better characterize the identity of the *NvPOU4*-expressing cells, we used double fluorescent *in situ* hybridization to test co-expression of *NvPOU4* with other genes expressed during neural development. We observed that *NvPOU4* is partially co-expressed with the neuropeptide gene *NvRFamide* (labeling differentiating sensory and ganglion cells; Figures 2A and 2B) and with *NvNcol3* (Figures 2C and 2D). In contrast, *NvPOU4* is not co-expressed with the neural progenitor marker *NvSoxB(2)* from blastula to late planula stages (Figures 2E, 2F, and S2; Videos S1–S9). As we have shown that the expression of *NvPOU4* depends on *NvSoxB(2)* function (Figures 1G–1K), the lack of co-expression of the two mRNAs indicates that they might be expressed sequentially in developing neurons. As a first step to test this possibility, we examined cell proliferation in *NvPOU4*-expressing cells. We incubated wild-type animals at late blastula

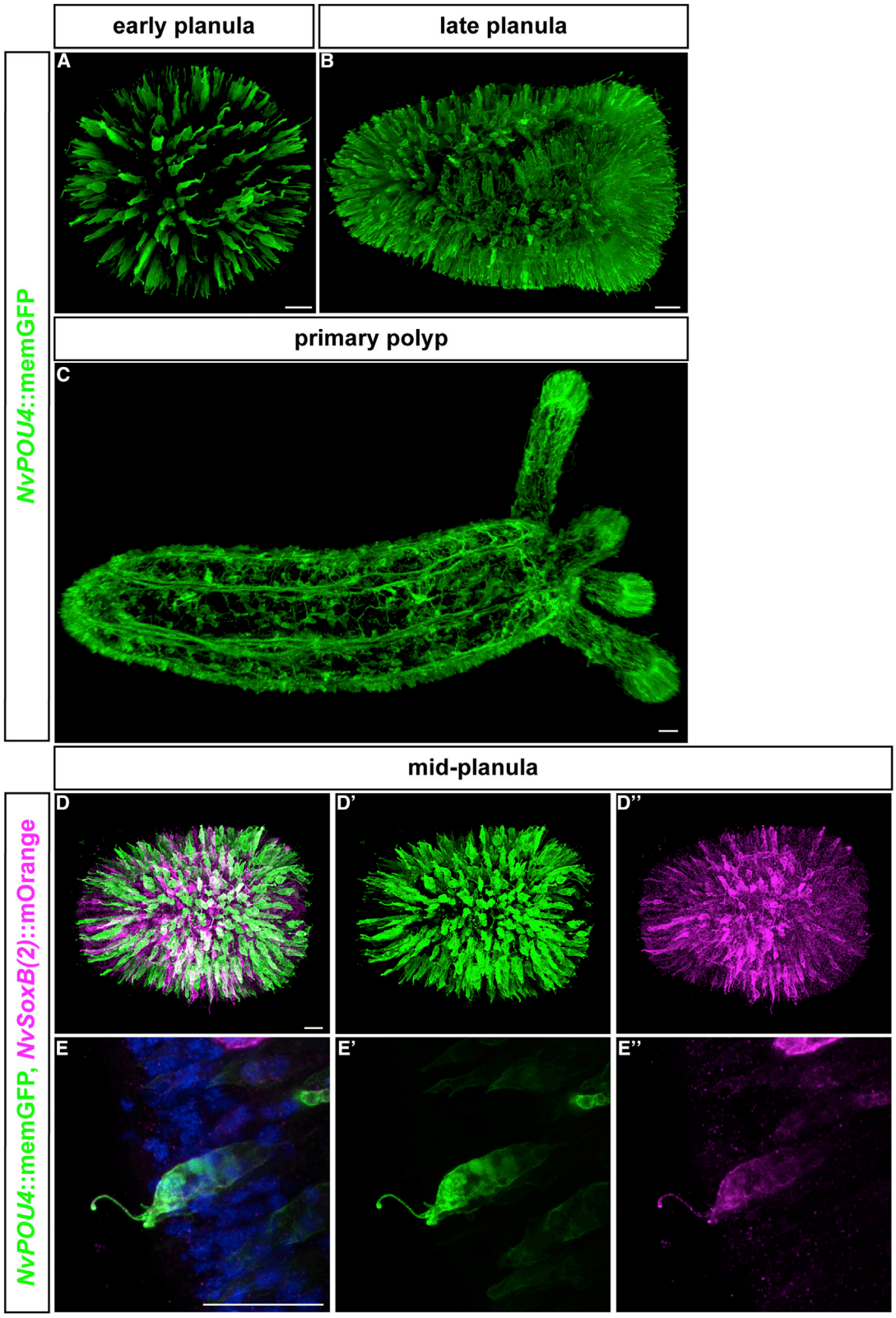

(legend on next page)

stage for 30 min with EdU, fixed them immediately afterward, and performed EdU detection together with fluorescence *in situ* hybridization (Figures 2G–2I; Video S10). We did not observe any EdU-positive, *NvPOU4*-expressing cells (10 embryos; in total, 310 *NvPOU4* expressing cells in 100 μm × 100 μm squares in the mid-lateral part of the blastoderm). This differs from previous observations of EdU-incorporating cells that express *NvSoxB(2)* mRNA (Richards and Rentzsch, 2014).

Together, these data suggest that *NvPOU4* is expressed in non-proliferating, differentiating cells of the developing nervous system.

NvPOU4-Expressing Cells Develop into Neurons and Cnidocytes

To gain further insight into the nature of the *NvPOU4*-expressing cells, we generated a stable transgenic reporter line, in which a 4.7-kb upstream region of the *NvPOU4* coding sequence drives the expression of a membrane-tethered GFP (*NvPOU4*::memGFP). This allowed the identification of the *NvPOU4*-expressing cells and their progeny. Double fluorescence *in situ* hybridization of *memGFP* and *NvPOU4* in transgenic embryos showed a strong co-expression of the reporter gene transcripts and endogenous *NvPOU4* (Figure S3); this confirms that the reporter line accurately reflects the endogenous expression of *NvPOU4*.

Analysis of memGFP expression showed that it starts in early gastrula and is increased and maintained until polyp stages (Figures 3A–3C). At early planula stage, memGFP is localized in scattered ectodermal cells that have a slender shape and often an apical cilium (Figure 3A). Later on, at late planula stage, it is possible to detect the memGFP protein in both scattered ectodermal and endodermal cells (Figure 3B). At primary polyp stage, memGFP localization highlights the nerve net and is expressed in cells with various morphologies in the ectoderm and in the endoderm. In the endoderm, neurites of many memGFP$^+$ neurons extend along the mesenteries—the longitudinal in foldings of the endoderm. At this stage, there is also expression of the memGFP protein in scattered ectodermal cells all over the body column and in the tentacles of the animals, with particularly strong labeling in the tips of the tentacles. This pattern of transgene expression is maintained in juvenile and adult polyps (not shown).

Next, we generated double transgenic animals by crossing the *NvPOU4*::memGFP line to other previously characterized neuronal reporter lines. To clarify the relationship between *NvSoxB(2)* and *NvPOU4*-expressing cells, we generated *NvSoxB(2)*::memOrange; *NvPOU4*::memGFP double transgenics. At both gastrula and planula stage, nearly all *NvPOU4*::memGFP cells were also labeled with the *NvSoxB(2)* reporter transgene (Figures 3D and 3E). This supports the scenario in which the two genes are expressed sequentially in the same cells, with *NvSoxB(2)* expression preceding that of *NvPOU4*. We also noted that the overlap of the two transgenes is not absolute: although the *NvSoxB(2)*::memOrange transgene is expressed more broadly, there are also some cells that are positive for *NvPOU4*::memGFP, but not for *NvSoxB(2)*::memOrange (Figure 3D).

The previously characterized *NvNcol3*::mOrange2 line labels differentiating cnidocysts—the extrusive capsules of the cnidocytes (Sunagar et al., 2018). In double transgenic animals (*NvPOU4*::memGFP, *NvNcol3*::mOrange2; Figures 4A–4F), GFP-positive membranes surround all mOrange2-positive cnidocysts throughout the animal from mid-planula to polyp stage. Most of the ectodermal memGFP$^+$ cells appear to contain a cnidocyst and are therefore differentiating or differentiated cnidocytes (Figures 4B, 4E, and 4F). However, this co-expression is not absolute, and some memGFP$^+$ cells do not contain a developing cnidocyst and have a long apical cilium (Figure 4C). The *NvPOU4* transgene is thus expressed in developing cnidocytes and potentially other cell types.

To gain further insight into the nature of these other *NvPOU4*-expressing cells, we generated *NvPOU4*::memGFP, *NvElav1*::mOrange double transgenic animals (Figures 4G–4L). The *NvElav1*::mOrange transgenic line labels a subset of sensory and ganglion cells, but not cnidocytes (Nakanishi et al., 2012). From early planula stage, we could note ectodermal cells that expressed both fluorescent proteins, suggesting that a subset of sensory cells expresses *NvPOU4* (Figures 4H and 4I). The co-expression of the two transgenes is more prominent at primary polyp stages, with much of the *NvElav1*::mOrange-positive endodermal nerve net also expressing the memGFP protein (Figures 4J–4L), including cells with the morphology of ganglion cells (arrow in Figure 4K′). We also generated double transgenics of *NvPOU4*::memGFP with the *NvFoxQ2d*::mOrange line, in which a small subpopulation of ectodermal sensory cells is labeled (Busengdal and Rentzsch, 2017). We did not observe co-expression of *NvPOU4*::memGFP with *NvFoxQ2d*::mOrange (data not shown).

Thus, the *NvPOU4* transgenic reporter line labels cnidocytes and a subset of sensory and ganglion cell types, and transgene expression is maintained at the polyp stage.

NvPOU4 Is Required for Neural Differentiation

To identify the function of *NvPOU4*, we generated a mutant line using the CRISPR/Cas9 system. We targeted the beginning of the POU domain with a single guide RNA (Figure 5A). Genotyping of F1 animals derived from one founder polyp revealed a prevalent deletion of 31 bp, causing a frameshift and a premature stop

Figure 3. A Transgenic Reporter Line Recapitulates the Expression of *NvPOU4*

(A–E) Confocal microscopy images of transgenic lines. (A–C). The *NvPOU4*::memGFP transgenic line; memGFP is detected by anti-GFP antibody (green). All images are lateral views with the aboral pole to the left. All images are Imaris snapshots from the 3D reconstructions. Expression of memGFP is detected from gastrula stage on and is consistent with the *in situ* hybridization signals (Figure S3).

(D and E) Double transgenic animals with *NvPOU4*::memGFP (green), *NvSoxB(2)*::mOrange (magenta), and nuclei (blue in E). Lateral views with aboral pole to the left are shown. At planula stage, the *NvPOU4*::memGFP$^+$ cells are also mOrange$^+$. (E)–(E″) shows a double-positive putative sensory cell in the ectoderm. Animals from at least three biological replicates (separate spawnings) were analyzed.

Scale bars represent 20 μm.

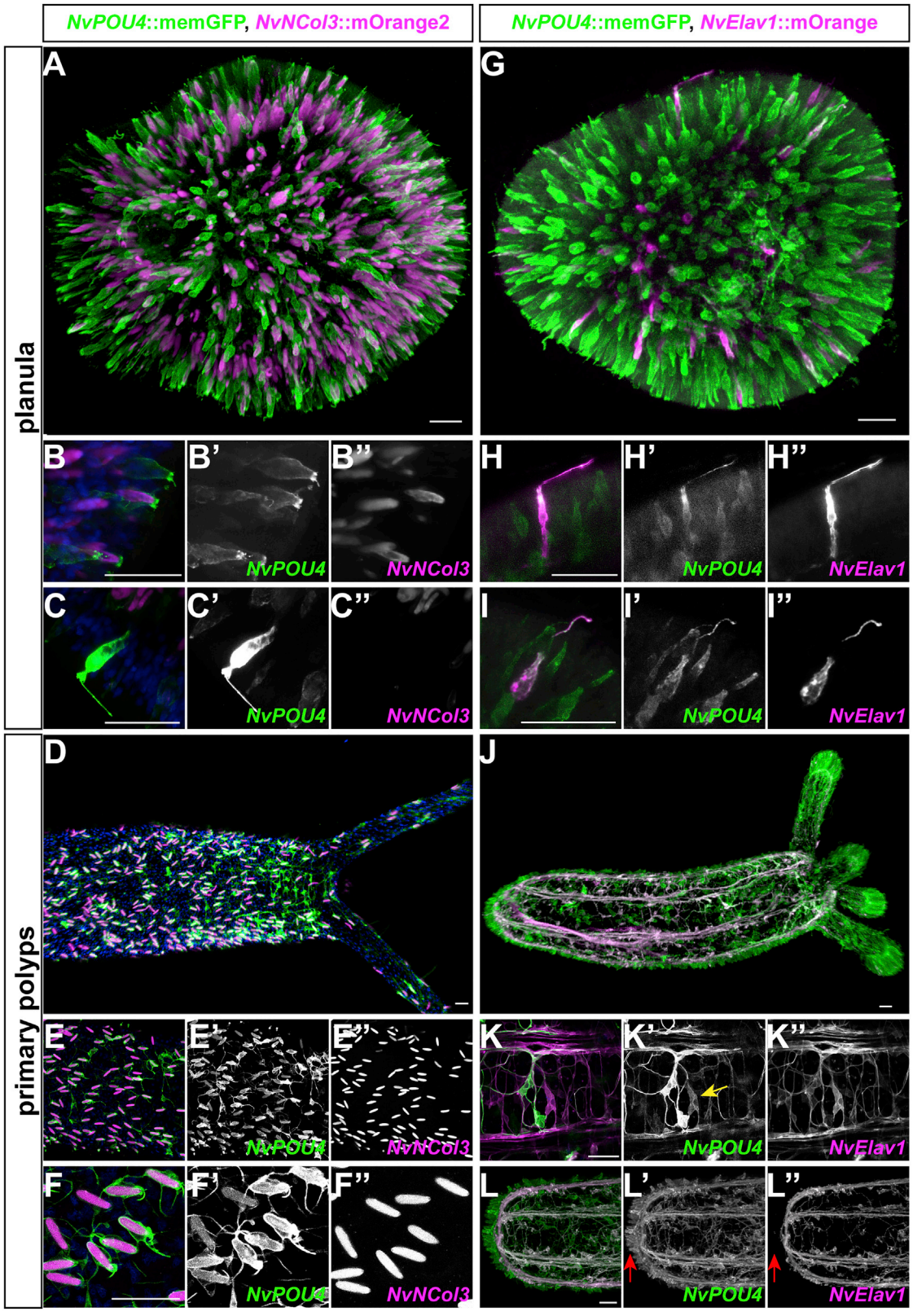

(legend on next page)

codon that truncates the encoded protein before the DNA binding domain (Figures 5A and S4). We denote this allele as *NvPOU4*^{1} and refer to it in the text as *NvPOU4*$^{-}$. We collected F1 animals with this 31-bp deletion and then crossed them to obtain 25% homozygous F2 mutants. Light microscopic observation of the F2 animals showed that 26% of them lacked elongated cnidocyst capsules at primary polyp stage (n = 97 animals). We extracted DNA and sequenced the *NvPOU4* gene of those animals and of their siblings that possessed cnidocysts (Figures 5B and 5C). This showed that 90% of the animals without cnidocysts were *NvPOU4*$^{-/-}$, whereas all sibling controls with cnidocysts were *NvPOU4*$^{+/+}$ or *NvPOU4*$^{+/-}$. This confirmed that *NvPOU4* homozygous mutants lack cnidocysts. These polyps were unable to catch prey and did not survive beyond the primary polyp stage. To better characterize the cnidocyte phenotype, we performed stainings to distinguish developing from mature cnidocytes. An antibody against NvNCol3 detects the cnidocysts throughout their development but does not detect the fully mature cnidocyst capsules (with very few exceptions; Babonis and Martindale, 2017; Zenkert et al., 2011). The matrix of the mature cnidocysts is specifically labeled by incubation with a high concentration of 4′,6-diamidino-2-phenylindole (DAPI) in the presence of EDTA (Szczepanek et al., 2002). We noticed that *NvPOU4*$^{-/-}$ polyps do have patches of NvNCol3 staining but lack any of the well-defined, elongated capsules that form during cnidocyte differentiation. Such capsules were neither visible by staining with the NvNCol3 antibody nor by the high concentration of DAPI (Figures 5D–5K). We confirmed this observation by generating *NvPOU4*$^{-/-}$, *NvNCol3*::mOrange2 animals; in these animals, NvNCol3 is expressed, but mature capsules fail to differentiate (Figure S4). The diffuse nature of NvNCol3 staining in the mutants made quantification of the stained cells difficult; thus, we cannot exclude an effect on the number of NvNCol3-expressing cells. These experiments suggest, however, that *NvPOU4* is primarily required for the terminal differentiation of cnidocytes in *Nematostella*.

We next studied the role of *NvPOU4* during the development of other neural cell types (ganglion and sensory cells) identified by the *NvPOU4*::memGFP reporter line. To do so, we generated *NvPOU4*$^{-/-}$, *NvElav1*::mOrange animals by crossing *NvPOU4*$^{+/-}$ to *NvPOU4*$^{+/-}$, *NvElav1*::mOrange polyps. We collected primary polyps with *NvElav1*::mOrange expression and inspected them for the cnidocyte phenotype. Despite a lack of mature cnidocytes, these putative *NvPOU4*$^{-/-}$, *NvElav1*::mOrange animals displayed no gross aberration of their *NvElav1*$^{+}$ nervous system (Figures 6A–6D). For quantification, we randomly imaged *NvElav1*::mOrange^{+} polyps, counted the number of mOrange^{+} cells in a 100 μm × 100 μm square in the body column and determined the presence or absence of mature cnidocytes by light microscopy *a posteriori*. We did not find a statistically significant difference in the number of mOrange^{+} cells between polyps with and without mature capsules, respectively (Figure S5). This suggests that *NvPOU4* does not have a major role in the specification or gross morphological development of the *NvElav1*$^{+}$ neurons.

Loss of *NvPOU4* Affects the Transcriptomes of *NvNCol3*- and *NvElav1*-Expressing Neural Cells

To characterize the function of *NvPOU4* in more detail, we decided to analyze transcriptional changes using RNA sequencing. We compared cnidocyst-lacking *NvPOU4*$^{-/-}$ animals at primary polyp stage and compared them to their cnidocyst-containing siblings (consisting of *NvPOU4*$^{+/+}$ and *NvPOU4*$^{+/-}$ animals). RNA sequencing of four biological replicates confirmed that *NvPOU4*$^{-/-}$ animals only generate transcripts of this gene with the 31-bp deletion (Figure S5). In total, 1,217 genes were differentially regulated (p-adjusted value < 0.05; no threshold for fold change), with 576 being down- and 641 being upregulated in the *NvPOU4*$^{-/-}$ polyps (Figure 6E; Table S1). An analysis of Gene Ontology (GO) terms identified 21 terms that are overrepresented among the downregulated genes, with "ion channel activity," "extracellular ligand-gated ion channel activity," "potassium channel activity," "acetylcholine binding," "calcium ion binding," and "voltage-gated potassium channel activity" being overrepresented in the GO domain "molecular function" (Figure 6F). The only term that is overrepresented among the upregulated genes is "endoplasmic reticulum" in the GO domain "cellular component." Although this is consistent with a role for *NvPOU4* in nervous system development, the low proportion of *Nematostella* genes that are associated with a GO term (39.4% of all differentially expressed genes) limits the power of the analysis.

Figure 4. *NvPOU4*::memGFP identifies neural cell types.

(A–F) Double transgenic animals with *NvPOU4*::memGFP (green), *NvNCol3*::mOrange2 (magenta), and DAPI in blue. Lateral view with aboral pole to the left.

(A–C) Planula stage.

(E and F) Live images at primary polyp stage.

(A, B, D, E, and F) From gastrula to primary polyp stage, the *NvNCol3*::mOrange2^{+} capsules are surrounded by the memGFP, suggesting that *NvPOU4*::memGFP identifies cnidocytes.

(C) Some *NvPOU4*::memGFP^{+} cells do not contain *NvNCol3*::mOrange2^{+} capsules, suggesting that the *NvPOU4*::memGFP line identifies cnidocytes and other cell types. In (B)–(C) and (E)–(F), *NvPOU4* and *NvNCol3* stand for *NvPOU4*::memGFP and *NvNCol3*::mOrange2, respectively. (A) and (D) are projections of stacks, and (B)–(C″) and (E)–(F″) are single confocal sections.

(G–L) Double transgenic animals with *NvPOU4*::memGFP (green) and *NvElav1*::mOrange (magenta). Lateral views with aboral pole to the left are shown.

(G–I) At planula stage, some ectodermal cells are positive for both reporter proteins; these cells have an apical cilium.

(J–L) At primary polyp stage, the endodermal nerve net expresses both fluorescent proteins. Arrow in (K′) indicates an endodermal cell with ganglion cell-like morphology.

(L) The cnidocytes (red arrows in L and L′) appear to be the only cells that do not co-express both transgenes. In (H)–(I) and (K)–(L), *NvPOU4* and *NvNCol3* stand for *NvPOU4*::memGFP and *NvNCol3*::mOrange2, respectively. (G) and (J) are projections of stacks, and (H)–(I″) and (K)–(L″) are single confocal sections. Animals from at least three biological replicates (separate spawnings) were analyzed.

Scale bars represent 20 μm.

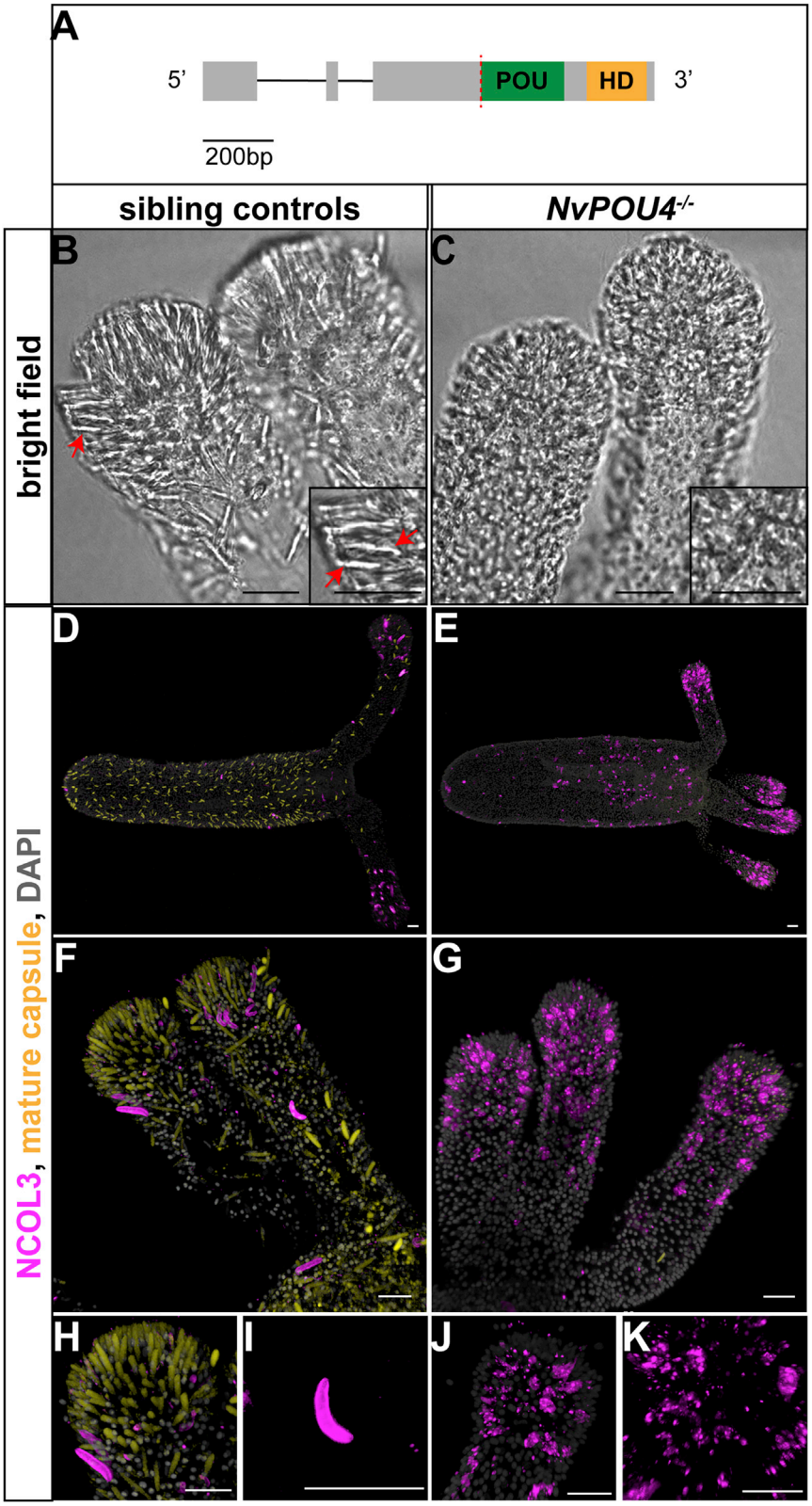

Figure 5. The Loss of *NvPOU4* Prevents Cnidocyte Differentiation

(A) Schematic of the CRISPR/Cas9 targeting strategy. Exons are in gray boxes, the POU domain is shown as a green box, and the homeodomain (HD) is shown as a yellow box. The sgRNA targets the start of the POU domain (red dashed line) and generated a deletion of 31 bp, causing a frameshift and the appearance of a premature STOP codon.

(B and C) Bright field picture of the tentacle tips of (B) primary polyps control (*NvPOU4*$^{+/+}$ and *NvPOU4*$^{+/-}$) versus (C) *NvPOU4*$^{-/-}$. Red arrows highlight elongated cnidocysts.

(D–K) Antibody staining of NvNCol3 (magenta), mature capsules (yellow), and nuclei (gray) in controls (D, F, H, and I) versus *NvPOU4*$^{-/-}$ (E, G, J, and K). *NvPOU4*$^{-/-}$ animals lack elongated mature capsules. They still show NvNCol3 antibody staining, suggesting that cnidocytes are specified but do not differentiate properly, highlighted by the shape of the NvNCol3-positive capsule (I and K). (D)–(K) are projections of stacks of confocal sections. Animals from at least three biological replicates (separate spawnings) were analyzed. Scale bars represent 20 μm.

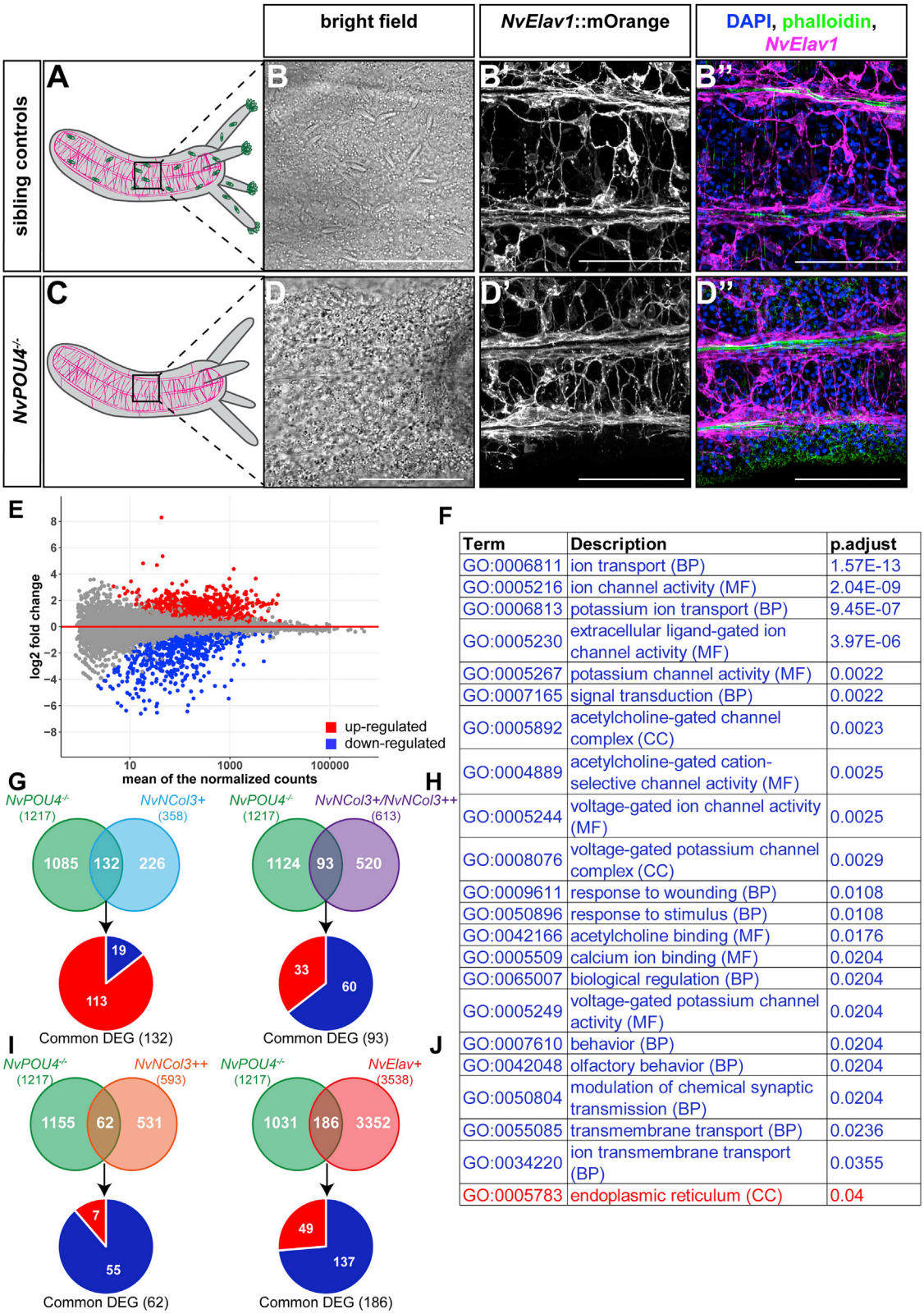

Term	Description	p.adjust
GO:0006811	ion transport (BP)	1.57E-13
GO:0005216	ion channel activity (MF)	2.04E-09
GO:0006813	potassium ion transport (BP)	9.45E-07
GO:0005230	extracellular ligand-gated ion channel activity (MF)	3.97E-06
GO:0005267	potassium channel activity (MF)	0.0022
GO:0007165	signal transduction (BP)	0.0022
GO:0005892	acetylcholine-gated channel complex (CC)	0.0023
GO:0004889	acetylcholine-gated cation-selective channel activity (MF)	0.0025
GO:0005244	voltage-gated ion channel activity (MF)	0.0025
GO:0008076	voltage-gated potassium channel complex (CC)	0.0029
GO:0009611	response to wounding (BP)	0.0108
GO:0050896	response to stimulus (BP)	0.0108
GO:0042166	acetylcholine binding (MF)	0.0176
GO:0005509	calcium ion binding (MF)	0.0204
GO:0065007	biological regulation (BP)	0.0204
GO:0005249	voltage-gated potassium channel activity (MF)	0.0204
GO:0007610	behavior (BP)	0.0204
GO:0042048	olfactory behavior (BP)	0.0204
GO:0050804	modulation of chemical synaptic transmission (BP)	0.0204
GO:0055085	transmembrane transport (BP)	0.0236
GO:0034220	ion transmembrane transport (BP)	0.0355
GO:0005783	endoplasmic reticulum (CC)	0.04

(legend on next page)

Our analysis of double transgenic animals has shown that separate subsets of *NvPOU4*-expressing cells give rise to *NvNCol3*- and *NvElav1*-expressing cells (Figure 4). We therefore used the transcriptomes of *NvNCol3*::mOrange^{+} (Sunagar et al., 2018) and *NvElav1*::mOrange^{+} cells enriched by fluorescence-activated cell sorting (FACS) to assign genes differentially regulated in *NvPOU4* mutants to these two different populations of neural cells. For the *NvNCol3*::mOrange^{+} cells, different levels of fluorescence combined with microscopic examination have previously been used to characterize two populations of these cells and to generate transcriptomes of them. One of the cell populations is enriched for differentiating cnidocytes (mOrange positive), and the other one consists of mature cnidocytes (mOrange super-positive, with higher fluorescence; Sunagar et al., 2018). Among the genes that were differentially expressed in *NvPOU4* mutants, we identified 287 genes that were in common with those reported in the *NvNCol3*::mOrange transcriptomes, with 132 genes being differentially expressed only in the positive cells, 62 only in the super-positive cells, and 93 in both groups of cells (Figures 6G–6I; Table S1). Interestingly, we noticed a striking difference in the proportion of up- and downregulated genes in these three groups of cells. Of the 132 differentially expressed genes (DEGs) present only in the mOrange-positive, differentiating cells, 113 (85.6%) were up- and 19 (14.4%) were downregulated (Figure 6G) in the *NvPOU4* mutants. In contrast, of the 62 DEGs only present in the mOrange super-positive, more mature cells, 55 (88.7%) were down- and only 7 (11.3%) were upregulated (Figure 6I). Of the 93 DEGs found in both groups of cells, 60 (64.5%) were down- and 33 (35.5%) were upregulated (Figure 6H). This suggests that mutation of *NvPOU4* reduces the expression of genes involved in the terminal differentiation of cnidocytes and increases the expression of genes involved in earlier steps of their development.

We next generated transcriptomes of *NvElav1*::mOrange-positive and negative cells at primary polyp stage and identified 3,538 genes with significantly higher expression level in *NvElav1*::mOrange-positive cells. Of these genes, a total of 186 were differentially regulated in *NvPOU4* mutants and, among them, 137 (73.7%) were downregulated but only 49 (26.3%) were upregulated in the mutants (Figure 6J). Thus, similar to the situation in the *NvNCol3*::mOrange super-positive cnidocytes, *NvPOU4* appears to function mainly as a positive regulator of genes expressed in *NvElav1*::mOrange-positive cells. The broad expression in *NvElav1*::mOrange^{+} neurons suggests that *NvPOU4* functions in the differentiation of different types of neurons. To support this hypothesis, we selected two genes that are downregulated in the *NvPOU4* mutants and are upregulated in *NvElav1*::mOrange-expressing cells for double fluorescentce *in situ* hybridization with *NvPOU4*. We found *Nve22966* (a putative ionotropic glutamate receptor) to be co-expressed with *NvPOU4* mainly in endodermal cells (Figures 7A and 7B), whereas the co-expression of *NvPOU4* and *Nve21438* (a putative $GABA_A$ receptor subunit) is most prominent in ectodermal cells (Figures 7C and 7D). This indicates that *NvPOU4* indeed contributes to the differentiation of different subpopulations of *NvElav1*::mOrange-expressing neurons.

Taken together, our transcriptome analyses show that *NvPOU4* is mainly required for the expression of genes that are expressed at late stages of cnidocyte and neuron differentiation. This is consistent with the morphological observations of the *NvPOU4* mutants in the background of the *NvNCol3*::mOrange2 and *NvElav1*::mOrange transgenic lines and suggests that *NvPOU4* regulates the terminal differentiation of neural cells.

DISCUSSION

In this report, we have shown that *NvPOU4* is expressed in postmitotic cells that are derived from *NvSoxB(2)*-expressing neural progenitor cells and give rise to cnidocytes, sensory cells, and ganglion cells. Despite its expression from blastula stage on, mutation of *NvPOU4* does not prevent the initial specification of these cells. Instead, our data suggest that the main function of *POU4* in *Nematostella vectensis* is the regulation of the terminal differentiation of neural cells.

Figure 6. Loss of *NvPOU4* Affects the Transcriptomes of *NvNCol3*- and *NvElav1*-Expressing Neural Cells

(A–D) *NvPOU4*$^{-/-}$ animals were distinguished based on the absence of cnidocyte capsules.(A) and (C) are graphic illustrations, (B) and (D) are light microscopic images of areas equivalent to the rectangles in (A) and (C).

(B′–D″) Confocal images of anti-dsRed antibody staining (detecting mOrange, shown in magenta) in *NvPOU4*$^{-/-}$, *NvElav1*::mOrange$^{+/-}$ polyps (D′ and D″; 10 dpf) and sibling controls (B′ and B″), phalloidin in green, and DAPI in blue. Scale bars represent 50 μm. This experiment suggested that the *NvElav1*$^{+}$ cells are specified properly in the absence of *NvPOU4.*

(E) MA plot of the RNA sequencing comparing *NvPOU4*$^{-/-}$ animals with their sibling control (selection based on the cnidocyte phenotype; four biological replicates). In total, 1,217 genes were differentially expressed (p-adjusted < 0.05; no minimal fold change), 641 were found upregulated (red), and 576 were found downregulated (blue).

(F) GO term analysis of the *NvPOU4*$^{-/-}$ versus siblings (with $p < 0.05$). GO terms overrepresented among downregulated genes are in blue, and those overrepresented among upregulated genes are in red.

(G and H) Comparison of the genes differentially expressed in *NvPOU4*$^{-/-}$ with the published *NvNCol3*::mOrange2 transcriptomes (Sunagar et al., 2018). *NvNCol3*$^{+}$ (positive) represents the genes expressed in differentiating cnidocytes (358), *NvNcol3*$^{+}$+ (super-positive) represents the genes expressed in fully differentiated cnidocytes (593), and *NvNcol3*$^{+}$/*NvNcol3*$^{++}$ represents the genes that are expressed in both differentiating and differentiated cnidocytes (613).

(G) 85.6% (113/132) of the differentially expressed genes (DEGs) common to the *NvPOU4* mutants and the *NvNcol3*$^{+}$ transcriptomes are upregulated in the *NvPOU4* mutants.

(H) 64.5% (60/93) of the differentially expressed genes common to *NvPOU4* mutants and the *NvNcol3*$^{+}$/*NvNcol3*$^{++}$ transcriptome are downregulated in the *NvPOU4* mutants.

(I) 85.6% (55/62) of the differentially expressed genes common to the *NvPOU4* mutant and the *NvNcol3*$^{++}$ transcriptome are downregulated in the *NvPOU4* mutants.

(J) Comparison of the genes differentially expressed in *NvPOU4*$^{-/-}$ with the *NvElav1*::mOrange transcriptome. 73.7% (137/186) of the differentially expressed genes common to *NvPOU4* mutant and the *NvElav1* transcriptome are downregulated in the *NvPOU4* mutants.

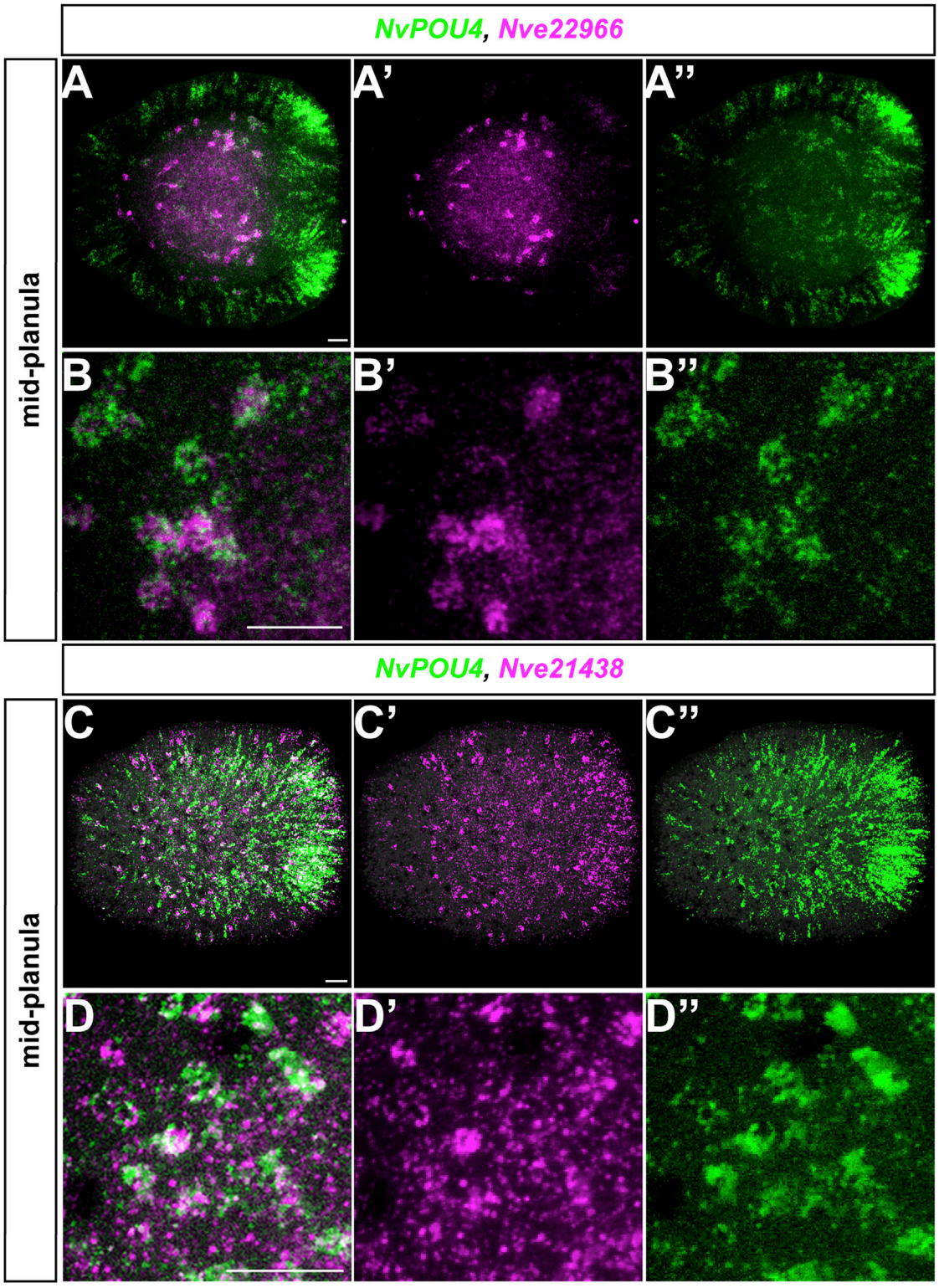

Figure 7. Co-expression of *NvPOU4* with Glutamate and $GABA_A$ Receptor Genes in Different Populations of Cells

(A–D) Lateral views of double fluorescence *in situ* hybridization with probes indicated on the top and the developmental stage on the left side.

(A and B) *NvPOU4* is labeled in green and *Nve22966* (a putative glutamate receptor) in magenta; co-expression is visible in an endodermal population of cells.

(legend continued on next page)

Cnidocyte precursors in *NvPOU4* mutants still produce NvNcol3 protein. They fail, however, to assemble the elongated cnidocysts characteristic of mature cnidocytes. This morphological observation suggested that, in these cells, *NvPOU4* mainly regulates the transcription of genes that encode factors required for the final steps of cnidocyte differentiation. The availability of separate transcriptomes enriched for cnidocytes at earlier stages (at or before the beginning of cnidocyst formation) and at later stages (containing elongated cnidocysts) of their development (Sunagar et al., 2018) allowed us to analyze the requirement for *NvPOU4* in this process in more detail. The preponderance of downregulation among genes that are specifically enriched in late-stage cnidocytes matched the observed lack of mature cnidocysts. In contrast, we did not expect that many of the genes that are specifically expressed in early-stage cnidocytes would be upregulated in *NvPOU4* mutants. This included the *NvNCol3* gene, *NvPaxA* (a transcription factor that positively regulates *NvNCol3* expression; Babonis and Martindale, 2017), and *NvPOU4* itself. A possible explanation is that the failure to produce functional cnidocytes leads to a "compensatory" response that increases the number of cells entering the cnidocyte differentiation pathway. An alternative, but not mutually exclusive, possibility is that *NvPOU4* is required for the downregulation of genes that are temporarily expressed at an earlier stage of cnidocyte differentiation, resulting in prolonged expression of these genes in *NvPOU4* mutants.

For the *NvElav1*::mOrange-expressing neurons, we currently cannot separate cells at different stages of their differentiation. At the primary polyp stage, all or almost all *NvElav1*::mOrange-positive neurons possess neurites and are thus either at a late stage of their development or terminally differentiated (Nakanishi et al., 2012). In homozygous *NvPOU4* mutants, there is no significant reduction in the number of *NvElav1*::mOrange-expressing neurons, and the neurons extend neurites that do not show gross morphological alterations or obviously aberrant projection patterns (Figures 6B′ and 6D′). These observations suggest that, in the *NvElav1*$^+$ endodermal neurons, *NvPOU4* mainly functions in terminal differentiation, regulating, for example, the repertoire of neurotransmitter receptors. In line with such a function, the expression levels of genes encoding glutamate, acetylcholine, and GABA receptors are reduced in *NvPOU4* mutants. We note, however, that *NvPOU4* may have other or additional roles in subpopulations of *NvElav1*-expressing neurons.

Of the 1,217 genes differentially expressed in *NvPOU4* mutants, only 287 are upregulated in the cnidocyte transcriptomes and 186 in the *NvElav1*::mOrange transcriptome. This is a surprising observation because the double transgenic lines suggest that the majority of *NvPOU4*::memGFP-expressing cells are included in the *NvNCol3*::mOrange or *NvElav1*::memOrange-positive cells. A possible explanation is the difference in the age of the polyps used for the isolation of cnidocytes (3 to 4 months; Sunagar et al., 2018) and the *NvPOU4* mutants (14 days). The proportion of different types of cnidocytes has been shown to differ between primary and adult polyps (Zenkert et al., 2011), and the cnidocyte transcriptomes may therefore lack genes that are expressed predominantly at earlier stages. Similarly, only cnidocytes from the tentacles were used for generating the cnidocyte transcriptomes, whereas *NvPOU4* is expressed in both tentacle and body column cnidocytes, and these regions have been shown to differ in the composition of cnidocyte types (Zenkert et al., 2011). Genes that are expressed in cnidocyte types that are more common in the body column (e.g., basitrichous haplonemas) may therefore be underrepresented in the cnidocyte transcriptomes. It will be interesting for future studies to understand whether additional populations of *NvPOU4*-expressing cells exist outside the *NvNCol3* and *NvElav1*$^+$ cells.

After functioning in neural development, POU4 genes have been shown to be required for the survival of several classes of neurons in *C. elegans* and in the mouse habenula (Serrano-Saiz et al., 2018). Deletion of *POU4* in these terminally differentiated neurons results in the loss of their neurotransmitter identity and their elimination by apoptosis (Serrano-Saiz et al., 2018), suggesting an evolutionarily conserved, post-developmental role for POU4 genes. Whether *NvPOU4* has a comparable role in *Nematostella* is currently not clear. A recent single-cell RNA sequencing study showed that *NvPOU4* is expressed in neural cells in adult animals (Sebé-Pedrós et al., 2018), allowing for a role in maintaining neural identity. We observed homozygous mutants until 20 days post-fertilization (they become primary polyps after 6 to 7 days) but did not detect alterations in the number or morphology of *NvElav1*::mOrange-positive neurons (data not shown). Due to the lack of cnidocytes, *NvPOU4* mutants are unable to catch prey and are thus not viable, which prevents long-term observations. Determining whether *NvPOU4* has a role in the maintenance of the identity of neurons will require the development of methods for conditional gene inactivation in *Nematostella*.

The *C. elegans* POU4 gene *unc-86* is a prime example of a terminal selector gene, and POU4 genes in other species have comparable functions in the terminal differentiation of neural cell types (Ayer and Carlson, 1991; Certel et al., 2000; Clyne et al., 1999; Duggan et al., 1998; Erkman et al., 2000; Gan et al., 1996; Gordon and Hobert, 2015; Huang et al., 1999, 2001; Serrano-Saiz et al., 2013; Sze et al., 2002). Terminal selectors act in a combinatorial manner to regulate terminal effector genes and determine cellular identity (Hobert, 2016). This allows individual transcription factors to act as terminal selectors in different types of neurons, for example, by cooperative binding to regulatory elements together with other transcription factors (Cho et al., 2014; Duggan et al., 1998; Wolfram et al., 2014; Xue et al., 1992). In *Nematostella*, single-cell RNA sequencing has revealed several *NvPOU4*-expressing "metacells" with overall neuron-like transcriptional profiles (Sebé-Pedrós et al.,

(C and D) *NvPOU4* is labeled in green and *Nve21438* (a putative $GABA_A$ receptor subunit) in magenta; co-expression is visible in an ectodermal population of cells. This suggests *NvPOU4* contributes to the differentiation of different subpopulations of *NvElav1*::mOrange$^+$ cells. Lateral views with the aboral pole to the left are shown. (A)–(A″) and (C)–(C″) are projections of stacks of confocal sections, and (B)–(B″) and (D)–(D″) are single confocal sections. *In situ* hybridizations were done on two biological replicates with n > 10 for each sample.
Scale bars represent 20 μm.

2018). Individual *NvPOU4*$^{+}$ metacells (likely representing different neural cell types) express different combinations of other transcription factors (Sebé-Pedrós et al., 2018), some of which may function together with *NvPOU4* in regulating the terminal differentiation of these cells. In line with this scenario, each of the *NvPOU4*$^{+}$ metacells expresses at least one transcription factor that has not been detected in any other *NvPOU4*$^{+}$ metacell (Table S1). Although the physical and functional interaction with other transcription factors and with regulatory elements of target genes remains to be explored in future work, the morphological and molecular analyses presented here support the hypothesis that *NvPOU4* acts as a terminal selector for different neural cell types in *Nematostella*.

The advent of single-cell sequencing technologies has led to the elaboration of concepts for the evolutionary diversification of cell types. Terminal selector genes are central to such concepts, as they are part of so-called "core regulatory complexes" (CoRCs), which regulate the cellular features that distinguish different cell types (Arendt et al., 2016). It has been hypothesized that evolutionary changes occur more slowly in core regulatory complexes than in terminal effector genes, which would make them more informative for inferring evolutionary relationships between cell types (Arendt et al., 2016, 2019). Our data show that, more than 600 million years after the divergence of the cnidarian and bilaterian lineages (dos Reis et al., 2015), POU4 genes function in the terminal differentiation of neural cells in cnidarians, as they do in bilaterians. *NvPOU4* regulates the terminal differentiation of strikingly different types of neural cells in *Nematostella*, the more "typical" *NvElav1*$^{+}$ neurons, and the highly derived, taxon-specific cnidocytes. This is likely due to cell-type-specific combinatorial regulation together with other transcription factors, and attempts to homologize POU4-expressing neural cell types will require a more detailed understanding of such combinatorial regulation. Nevertheless, we propose that the function of *NvPOU4* is derived from an ancestral function of POU4 genes as regulators of terminal neural differentiation. We cannot exclude, however, that, in some cases, POU4 genes have been co-opted into comparable roles in different cell types.

In summary, the observation that *NvPOU4* functions in the terminal differentiation of neural cells in *Nematostella* supports the hypothesis that the regulation of neurogenesis by conserved terminal selector genes is an ancient feature of nervous system development.

STAR★METHODS

Detailed methods are provided in the online version of this paper and include the following:

SUPPLEMENTAL INFORMATION

Supplemental Information can be found online at https://doi.org/10.1016/j.celrep.2020.03.031.

ACKNOWLEDGMENTS

We thank James Gahan and Marta Iglesias for generating the *NvElav1*::mOrange samples for RNA sequencing, Suat Özbek (COS Heidelberg) for the NvNCol3 antibody, James Gahan for critical reading of the manuscript, Eilen Myrvold and Lavina Jubek for excellent care of the Sars Centre *Nematostella* facility, and Ivan Kouzel for help with data visualization and statistics. Clemens Döring provided advice on Imaris and Malalaniaina Rakotobe helped with initial cloning and *in situ* hybridizations. Sequencing of the *NvPOU4* mutant and sibling transcriptomes was performed at the Norwegian Sequencing Centre (Oslo), and sequencing of the *NvElav1*::mOrange transcriptome was performed at EMBL GeneCore (Heidelberg). Cell sorting was performed at the Flow Cytometry Core Facility, Department of Clinical Science, University of Bergen. Bioinformatic analyses were supported by Elixir Norway. The work was funded by the Sars Centre Core budget and by a grant from the Research Council of Norway and the University of Bergen (251185/F20) to F.R., work in the Moran group was supported by grant 869/18 of the Israel Science Foundation to Y.M., and K.S. was supported by a Marie Skłodowska-Curie Fellowship and funding from the DBT-IISc Partnership Program.

AUTHOR CONTRIBUTIONS

O.T. designed and performed the experimental work, analyzed the data, contributed to the conceptualization, generated the figures, and wrote the manuscript. D.D. analyzed the transcriptome data. G.S.R. performed initial expression analysis of *NvPOU4* and provided supervision in the beginning of the project. K.S., Y.Y.C.-S., and Y.M. generated the *NvNCol3::mOrange2* transgenic line and shared it prior to publication. F.R. conceptualized and supervised the study and wrote the manuscript. All authors commented on the manuscript.

DECLARATION OF INTERESTS

The authors declare no competing interests.

Received: September 23, 2019
Revised: January 8, 2020
Accepted: March 11, 2020
Published: March 31, 2020

REFERENCES

Allan, D.W., and Thor, S. (2015). Transcriptional selectors, masters, and combinatorial codes: regulatory principles of neural subtype specification. Wiley Interdiscip. Rev. Dev. Biol. *4*, 505–528.

Anders, S., Pyl, P.T., and Huber, W. (2015). HTSeq–a Python framework to work with high-throughput sequencing data. Bioinformatics *31*, 166–169.

Arendt, D., Musser, J.M., Baker, C.V.H., Bergman, A., Cepko, C., Erwin, D.H., Pavlicev, M., Schlosser, G., Widder, S., Laubichler, M.D., and Wagner, G.P. (2016). The origin and evolution of cell types. Nat. Rev. Genet. *17*, 744–757.

Arendt, D., Bertucci, P.Y., Achim, K., and Musser, J.M. (2019). Evolution of neuronal types and families. Curr. Opin. Neurobiol. *56*, 144–152.

Ayer, R.K., Jr., and Carlson, J. (1991). acj6: a gene affecting olfactory physiology and behavior in Drosophila. Proc. Natl. Acad. Sci. USA *88*, 5467–5471.

Babonis, L.S., and Martindale, M.Q. (2017). *PaxA*, but not *PaxC*, is required for cnidocyte development in the sea anemone *Nematostella vectensis*. Evodevo *8*, 14.

Backfisch, B., Veedin Rajan, V.B., Fischer, R.M., Lohs, C., Arboleda, E., Tessmar-Raible, K., and Raible, F. (2013). Stable transgenesis in the marine annelid Platynereis dumerilii sheds new light on photoreceptor evolution. Proc. Natl. Acad. Sci. USA *110*, 193–198.

Badea, T.C., Cahill, H., Ecker, J., Hattar, S., and Nathans, J. (2009). Distinct roles of transcription factors brn3a and brn3b in controlling the development, morphology, and function of retinal ganglion cells. Neuron *61*, 852–864.

Badea, T.C., Williams, J., Smallwood, P., Shi, M., Motajo, O., and Nathans, J. (2012). Combinatorial expression of Brn3 transcription factors in somatosensory neurons: genetic and morphologic analysis. J. Neurosci. *32*, 995–1007.

Bolger, A.M., Lohse, M., and Usadel, B. (2014). Trimmomatic: a flexible trimmer for Illumina sequence data. Bioinformatics *30*, 2114–2120.

Busengdal, H., and Rentzsch, F. (2017). Unipotent progenitors contribute to the generation of sensory cell types in the nervous system of the cnidarian Nematostella vectensis. Dev. Biol. *431*, 59–68.

Candiani, S., Pennati, R., Oliveri, D., Locascio, A., Branno, M., Castagnola, P., Pestarino, M., and De Bernardi, F. (2005). Ci-POU-IV expression identifies PNS neurons in embryos and larvae of the ascidian Ciona intestinalis. Dev. Genes Evol. *215*, 41–45.

Candiani, S., Oliveri, D., Parodi, M., Bertini, E., and Pestarino, M. (2006). Expression of AmphiPOU-IV in the developing neural tube and epidermal sensory neural precursors in amphioxus supports a conserved role of class IV POU genes in the sensory cells development. Dev. Genes Evol. *216*, 623–633.

Certel, S.J., Clyne, P.J., Carlson, J.R., and Johnson, W.A. (2000). Regulation of central neuron synaptic targeting by the Drosophila POU protein, Acj6. Development *127*, 2395–2405.

Chalfie, M., Horvitz, H.R., and Sulston, J.E. (1981). Mutations that lead to reiterations in the cell lineages of C. elegans. Cell *24*, 59–69.

Cho, H.H., Cargnin, F., Kim, Y., Lee, B., Kwon, R.J., Nam, H., Shen, R., Barnes, A.P., Lee, J.W., Lee, S., and Lee, S.K. (2014). Isl1 directly controls a cholinergic neuronal identity in the developing forebrain and spinal cord by forming cell type-specific complexes. PLoS Genet. *10*, e1004280.

Clyne, P.J., Certel, S.J., de Bruyne, M., Zaslavsky, L., Johnson, W.A., and Carlson, J.R. (1999). The odor specificities of a subset of olfactory receptor neurons are governed by Acj6, a POU-domain transcription factor. Neuron *22*, 339–347.

Collum, R.G., Fisher, P.E., Datta, M., Mellis, S., Thiele, C., Huebner, K., Croce, C.M., Israel, M.A., Theil, T., Moroy, T., et al. (1992). A novel POU homeodomain gene specifically expressed in cells of the developing mammalian nervous system. Nucleic Acids Res. *20*, 4919–4925.

Dobin, A., Davis, C.A., Schlesinger, F., Drenkow, J., Zaleski, C., Jha, S., Batut, P., Chaisson, M., and Gingeras, T.R. (2013). STAR: ultrafast universal RNA-seq aligner. Bioinformatics *29*, 15–21.

Doe, C.Q. (2008). Neural stem cells: balancing self-renewal with differentiation. Development *135*, 1575–1587.

dos Reis, M., Thawornwattana, Y., Angelis, K., Telford, M.J., Donoghue, P.C., and Yang, Z. (2015). Uncertainty in the timing of origin of animals and the limits of precision in molecular timescales. Curr. Biol. *25*, 2939–2950.

Duggan, A., Ma, C., and Chalfie, M. (1998). Regulation of touch receptor differentiation by the Caenorhabditis elegans mec-3 and unc-86 genes. Development *125*, 4107–4119.

Dunn, C.W., Giribet, G., Edgecombe, G.D., and Hejnol, A. (2014). Animal phylogeny and its evolutionary implications. Annu. Rev. Ecol. Evol. Syst. *45*, 371–395.

Edlund, T., and Jessell, T.M. (1999). Progression from extrinsic to intrinsic signaling in cell fate specification: a view from the nervous system. Cell *96*, 211–224.

Erkman, L., McEvilly, R.J., Luo, L., Ryan, A.K., Hooshmand, F., O'Connell, S.M., Keithley, E.M., Rapaport, D.H., Ryan, A.F., and Rosenfeld, M.G. (1996). Role of transcription factors Brn-3.1 and Brn-3.2 in auditory and visual system development. Nature *381*, 603–606.

Erkman, L., Yates, P.A., McLaughlin, T., McEvilly, R.J., Whisenhunt, T., O'Connell, S.M., Krones, A.I., Kirby, M.A., Rapaport, D.H., Bermingham, J.R., et al. (2000). A POU domain transcription factor-dependent program regulates axon pathfinding in the vertebrate visual system. Neuron *28*, 779–792.

Ernsberger, U. (2012). Regulation of gene expression during early neuronal differentiation: evidence for patterns conserved across neuron populations and vertebrate classes. Cell Tissue Res. *348*, 1–27.

Etchberger, J.F., Lorch, A., Sleumer, M.C., Zapf, R., Jones, S.J., Marra, M.A., Holt, R.A., Moerman, D.G., and Hobert, O. (2007). The molecular signature and cis-regulatory architecture of a C. elegans gustatory neuron. Genes Dev. *21*, 1653–1674.

Fedtsova, N.G., and Turner, E.E. (1995). Brn-3.0 expression identifies early post-mitotic CNS neurons and sensory neural precursors. Mech. Dev. *53*, 291–304.

Finney, M., and Ruvkun, G. (1990). The unc-86 gene product couples cell lineage and cell identity in C. elegans. Cell *63*, 895–905.

Fritzenwanker, J.H., and Technau, U. (2002). Induction of gametogenesis in the basal cnidarian Nematostella vectensis(Anthozoa). Dev. Genes Evol. *212*, 99–103.

Galliot, B., Quiquand, M., Ghila, L., de Rosa, R., Miljkovic-Licina, M., and Chera, S. (2009). Origins of neurogenesis, a cnidarian view. Dev. Biol. *332*, 2–24.

Gan, L., Xiang, M., Zhou, L., Wagner, D.S., Klein, W.H., and Nathans, J. (1996). POU domain factor Brn-3b is required for the development of a large set of retinal ganglion cells. Proc. Natl. Acad. Sci. USA *93*, 3920–3925.

Gerrero, M.R., McEvilly, R.J., Turner, E., Lin, C.R., O'Connell, S., Jenne, K.J., Hobbs, M.V., and Rosenfeld, M.G. (1993). Brn-3.0: a POU-domain protein expressed in the sensory, immune, and endocrine systems that functions on elements distinct from known octamer motifs. Proc. Natl. Acad. Sci. USA *90*, 10841–10845.

Gold, D.A., Gates, R.D., and Jacobs, D.K. (2014). The early expansion and evolutionary dynamics of POU class genes. Mol. Biol. Evol. *31*, 3136–3147.

Gordon, P.M., and Hobert, O. (2015). A competition mechanism for a homeotic neuron identity transformation in C. elegans. Dev. Cell *34*, 206–219.

Hand, C., and Uhlinger, K.R. (1992). The culture, sexual and asexual reproduction, and growth of the sea anemone *Nematostella vectensis*. Biol. Bull. *182*, 169–176.

Hennig, B.P., Velten, L., Racke, I., Tu, C.S., Thoms, M., Rybin, V., Besir, H., Remans, K., and Steinmetz, L.M. (2018). Large-scale low-cost NGS library preparation using a robust Tn5 purification and tagmentation protocol. G3 (Bethesda) *8*, 79–89.

Hobert, O. (2016). Terminal selectors of neuronal identity. Curr. Top. Dev. Biol. *116*, 455–475.

Hobert, O., and Kratsios, P. (2019). Neuronal identity control by terminal selectors in worms, flies, and chordates. Curr. Opin. Neurobiol. *56*, 97–105.

Homem, C.C., Repic, M., and Knoblich, J.A. (2015). Proliferation control in neural stem and progenitor cells. Nat. Rev. Neurosci. *16*, 647–659.

Hroudova, M., Vojta, P., Strnad, H., Krejcik, Z., Ridl, J., Paces, J., Vlcek, C., and Paces, V. (2012). Diversity, phylogeny and expression patterns of Pou

and Six homeodomain transcription factors in hydrozoan jellyfish Craspedacusta sowerbyi. PLoS ONE *7*, e36420.

Huang, E.J., Zang, K., Schmidt, A., Saulys, A., Xiang, M., and Reichardt, L.F. (1999). POU domain factor Brn-3a controls the differentiation and survival of trigeminal neurons by regulating Trk receptor expression. Development *126*, 2869–2882.

Huang, E.J., Liu, W., Fritzsch, B., Bianchi, L.M., Reichardt, L.F., and Xiang, M. (2001). Brn3a is a transcriptional regulator of soma size, target field innervation and axon pathfinding of inner ear sensory neurons. Development *128*, 2421–2432.

Ikmi, A., McKinney, S.A., Delventhal, K.M., and Gibson, M.C. (2014). TALEN and CRISPR/Cas9-mediated genome editing in the early-branching metazoan Nematostella vectensis. Nat. Commun. *5*, 5486.

Kraus, Y., Aman, A., Technau, U., and Genikhovich, G. (2016). Pre-bilaterian origin of the blastoporal axial organizer. Nat. Commun. *7*, 11694.

Larroux, C., Luke, G.N., Koopman, P., Rokhsar, D.S., Shimeld, S.M., and Degnan, B.M. (2008). Genesis and expansion of metazoan transcription factor gene classes. Mol. Biol. Evol. *25*, 980–996.

Layden, M.J., and Martindale, M.Q. (2014). Non-canonical Notch signaling represents an ancestral mechanism to regulate neural differentiation. Evodevo *5*, 30.

Layden, M.J., Boekhout, M., and Martindale, M.Q. (2012). Nematostella vectensis achaete-scute homolog NvashA regulates embryonic ectodermal neurogenesis and represents an ancient component of the metazoan neural specification pathway. Development *139*, 1013–1022.

Layden, M.J., Rentzsch, F., and Röttinger, E. (2016). The rise of the starlet sea anemone Nematostella vectensis as a model system to investigate development and regeneration. Wiley Interdiscip. Rev. Dev. Biol. *5*, 408–428.

Li, H., Handsaker, B., Wysoker, A., Fennell, T., Ruan, J., Homer, N., Marth, G., Abecasis, G., and Durbin, R.; 1000 Genome Project Data Processing Subgroup (2009). The Sequence Alignment/Map format and SAMtools. Bioinformatics *25*, 2078–2079.

Love, M.I., Huber, W., and Anders, S. (2014). Moderated estimation of fold change and dispersion for RNA-seq data with DESeq2. Genome Biol. *15*, 550.

Magie, C.R., Pang, K., and Martindale, M.Q. (2005). Genomic inventory and expression of Sox and Fox genes in the cnidarian Nematostella vectensis. Dev. Genes Evol. *215*, 618–630.

Marlow, H.Q., Srivastava, M., Matus, D.Q., Rokhsar, D., and Martindale, M.Q. (2009). Anatomy and development of the nervous system of Nematostella vectensis, an anthozoan cnidarian. Dev. Neurobiol. *69*, 235–254.

McEvilly, R.J., Erkman, L., Luo, L., Sawchenko, P.E., Ryan, A.F., and Rosenfeld, M.G. (1996). Requirement for Brn-3.0 in differentiation and survival of sensory and motor neurons. Nature *384*, 574–577.

Nakanishi, N., Yuan, D., Hartenstein, V., and Jacobs, D.K. (2010). Evolutionary origin of rhopalia: insights from cellular-level analyses of Otx and POU expression patterns in the developing rhopalial nervous system. Evol. Dev. *12*, 404–415.

Nakanishi, N., Renfer, E., Technau, U., and Rentzsch, F. (2012). Nervous systems of the sea anemone Nematostella vectensis are generated by ectoderm and endoderm and shaped by distinct mechanisms. Development *139*, 347–357.

Ninkina, N.N., Stevens, G.E., Wood, J.N., and Richardson, W.D. (1993). A novel Brn3-like POU transcription factor expressed in subsets of rat sensory and spinal cord neurons. Nucleic Acids Res. *21*, 3175–3182.

Nomaksteinsky, M., Kassabov, S., Chettouh, Z., Stoeklé, H.C., Bonnaud, L., Fortin, G., Kandel, E.R., and Brunet, J.F. (2013). Ancient origin of somatic and visceral neurons. BMC Biol. *11*, 53.

O'Brien, E.K., and Degnan, B.M. (2002). Developmental expression of a class IV POU gene in the gastropod Haliotis asinina supports a conserved role in sensory cell development in bilaterians. Dev. Genes Evol. *212*, 394–398.

Park, E., Hwang, D.S., Lee, J.S., Song, J.I., Seo, T.K., and Won, Y.J. (2012). Estimation of divergence times in cnidarian evolution based on mitochondrial protein-coding genes and the fossil record. Mol. Phylogenet. Evol. *62*, 329–345.

Picelli, S., Faridani, O.R., Björklund, A.K., Winberg, G., Sagasser, S., and Sandberg, R. (2014). Full-length RNA-seq from single cells using Smart-seq2. Nat. Protoc. *9*, 171–181.

Putnam, N.H., Srivastava, M., Hellsten, U., Dirks, B., Chapman, J., Salamov, A., Terry, A., Shapiro, H., Lindquist, E., Kapitonov, V.V., et al. (2007). Sea anemone genome reveals ancestral eumetazoan gene repertoire and genomic organization. Science *317*, 86–94.

Ramachandra, N.B., Gates, R.D., Ladurner, P., Jacobs, D.K., and Hartenstein, V. (2002). Embryonic development in the primitive bilaterian Neochildia fusca: normal morphogenesis and isolation of POU genes Brn-1 and Brn-3. Dev. Genes Evol. *212*, 55–69.

Renfer, E., and Technau, U. (2017). Meganuclease-assisted generation of stable transgenics in the sea anemone Nematostella vectensis. Nat. Protoc. *12*, 1844–1854.

Rentzsch, F., Layden, M., and Manuel, M. (2017). The cellular and molecular basis of cnidarian neurogenesis. Wiley Interdiscip. Rev. Dev. Biol. *6*, e257.

Rentzsch, F., Juliano, C., and Galliot, B. (2019). Modern genomic tools reveal the structural and cellular diversity of cnidarian nervous systems. Curr. Opin. Neurobiol. *56*, 87–96.

Richards, G.S., and Rentzsch, F. (2014). Transgenic analysis of a SoxB gene reveals neural progenitor cells in the cnidarian Nematostella vectensis. Development *141*, 4681–4689.

Richards, G.S., and Rentzsch, F. (2015). Regulation of Nematostella neural progenitors by SoxB, Notch and bHLH genes. Development *142*, 3332–3342.

Ryan, A.K., and Rosenfeld, M.G. (1997). POU domain family values: flexibility, partnerships, and developmental codes. Genes Dev. *11*, 1207–1225.

Sebé-Pedrós, A., Saudemont, B., Chomsky, E., Plessier, F., Mailhé, M.P., Renno, J., Loe-Mie, Y., Lifshitz, A., Mukamel, Z., Schmutz, S., et al. (2018). Cnidarian cell type diversity and regulation revealed by whole-organism single-cell RNA-seq. Cell *173*, 1520–1534.e20.

Serrano-Saiz, E., Poole, R.J., Felton, T., Zhang, F., De La Cruz, E.D., and Hobert, O. (2013). Modular control of glutamatergic neuronal identity in C. elegans by distinct homeodomain proteins. Cell *155*, 659–673.

Serrano-Saiz, E., Leyva-Diaz, E., De La Cruz, E., and Hobert, O. (2018). BRN3-type POU homeobox genes maintain the identity of mature postmitotic neurons in nematodes and mice. Curr. Biol. *28*, 2813–2823.e2.

Siebert, S., Farrell, J.A., Cazet, J.F., Abeykoon, Y., Primack, A.S., Schnitzler, C.E., and Juliano, C.E. (2019). Stem cell differentiation trajectories in *Hydra* resolved at single-cell resolution. Science *365*, eaav9314.

Stefanakis, N., Carrera, I., and Hobert, O. (2015). Regulatory logic of pan-neuronal gene expression in C. elegans. Neuron *87*, 733–750.

Stratmann, J., Ekman, H., and Thor, S. (2019). A branching gene regulatory network dictating different aspects of a neuronal cell identity. Development *146*, dev174300.

Sunagar, K., Columbus-Shenkar, Y.Y., Fridrich, A., Gutkovich, N., Aharoni, R., and Moran, Y. (2018). Cell type-specific expression profiling unravels the development and evolution of stinging cells in sea anemone. BMC Biol. *16*, 108.

Szczepanek, S., Cikala, M., and David, C.N. (2002). Poly-gamma-glutamate synthesis during formation of nematocyst capsules in Hydra. J. Cell Sci. *115*, 745–751.

Sze, J.Y., Zhang, S., Li, J., and Ruvkun, G. (2002). The C. elegans POU-domain transcription factor UNC-86 regulates the tph-1 tryptophan hydroxylase gene and neurite outgrowth in specific serotonergic neurons. Development *129*, 3901–3911.

Taverna, E., Götz, M., and Huttner, W.B. (2014). The cell biology of neurogenesis: toward an understanding of the development and evolution of the neocortex. Annu. Rev. Cell Dev. Biol. *30*, 465–502.

Telford, M.J., Budd, G.E., and Philippe, H. (2015). Phylogenomic insights into animal evolution. Curr. Biol. *25*, R876–R887.

Torres-Méndez, A., Bonnal, S., Marquez, Y., Roth, J., Iglesias, M., Permanyer, J., Almudí, I., O'Hanlon, D., Guitart, T., Soller, M., et al. (2019). A novel protein domain in an ancestral splicing factor drove the evolution of neural microexons. Nat. Ecol. Evol. *3*, 691–701.

Treacy, M.N., Neilson, L.I., Turner, E.E., He, X., and Rosenfeld, M.G. (1992). Twin of I-POU: a two amino acid difference in the I-POU homeodomain distinguishes an activator from an inhibitor of transcription. Cell *68*, 491–505.

Turner, E.E., Jenne, K.J., and Rosenfeld, M.G. (1994). Brn-3.2: a Brn-3-related transcription factor with distinctive central nervous system expression and regulation by retinoic acid. Neuron *12*, 205–218.

Watanabe, H., Fujisawa, T., and Holstein, T.W. (2009). Cnidarians and the evolutionary origin of the nervous system. Dev. Growth Differ. *51*, 167–183.

Wolfram, V., Southall, T.D., Günay, C., Prinz, A.A., Brand, A.H., and Baines, R.A. (2014). The transcription factors islet and Lim3 combinatorially regulate ion channel gene expression. J. Neurosci. *34*, 2538–2543.

Wollesen, T., McDougall, C., Degnan, B.M., and Wanninger, A. (2014). POU genes are expressed during the formation of individual ganglia of the cephalopod central nervous system. Evodevo *5*, 41.

Xiang, M., Zhou, L., Peng, Y.W., Eddy, R.L., Shows, T.B., and Nathans, J. (1993). Brn-3b: a POU domain gene expressed in a subset of retinal ganglion cells. Neuron *11*, 689–701.

Xiang, M., Zhou, L., Macke, J.P., Yoshioka, T., Hendry, S.H., Eddy, R.L., Shows, T.B., and Nathans, J. (1995). The Brn-3 family of POU-domain factors: primary structure, binding specificity, and expression in subsets of retinal ganglion cells and somatosensory neurons. J. Neurosci. *15*, 4762–4785.

Xiang, M., Gan, L., Zhou, L., Klein, W.H., and Nathans, J. (1996). Targeted deletion of the mouse POU domain gene Brn-3a causes selective loss of neurons in the brainstem and trigeminal ganglion, uncoordinated limb movement, and impaired suckling. Proc. Natl. Acad. Sci. USA *93*, 11950–11955.

Xiang, M., Gan, L., Li, D., Chen, Z.Y., Zhou, L., O'Malley, B.W., Jr., Klein, W., and Nathans, J. (1997). Essential role of POU-domain factor Brn-3c in auditory and vestibular hair cell development. Proc. Natl. Acad. Sci. USA *94*, 9445–9450.

Xue, D., Finney, M., Ruvkun, G., and Chalfie, M. (1992). Regulation of the mec-3 gene by the C.elegans homeoproteins UNC-86 and MEC-3. EMBO J. *11*, 4969–4979.

Yu, G., Wang, L.G., Han, Y., and He, Q.Y. (2012). clusterProfiler: an R package for comparing biological themes among gene clusters. OMICS *16*, 284–287.

Zenkert, C., Takahashi, T., Diesner, M.O., and Özbek, S. (2011). Morphological and molecular analysis of the Nematostella vectensis cnidom. PLoS ONE *6*, e22725.

Zhang, F., Bhattacharya, A., Nelson, J.C., Abe, N., Gordon, P., Lloret-Fernandez, C., Maicas, M., Flames, N., Mann, R.S., Colón-Ramos, D.A., and Hobert, O. (2014). The LIM and POU homeobox genes ttx-3 and unc-86 act as terminal selectors in distinct cholinergic and serotonergic neuron types. Development *141*, 422–435.

STAR★METHODS

KEY RESOURCES TABLE

REAGENT or RESOURCE	SOURCE	IDENTIFIER
Antibodies		
Guinea pig anti *Nematostella* NCol3	Provided by Suat Özbek, Heidelberg	N/A
Rabbit anti dsRed	Clontech	Cat# 632496; RRID: AB_10013483
Mouse anti GFP	Abcam	Cat# 1218; RRID: AB_298911
Biological Samples		
NvPOU4 homozygous mutants	this study	N/A
Siblings of *NvPOU4* homozygous mutants (+/− and +/+)	this study	N/A
Critical Commercial Assays		
Click-iT EdU Cell proliferation kit	Thermo Scientific/ Molecular Probes	Cat# C10337
TruSeq® stranded mRNA library kit	Illumina	Cat# 20020594
TSA plus fluorescein kit	Perkin Elmer	Cat# NEL741001KT
TSA plus Cyanine 3 kit	Perkin Elmer	Cat# NEL744001KT
Deposited Data		
NvPOU4 mutant transcriptome at 12dpf	ArrayExpress https://www.ebi.ac.uk/arrayexpress/	E-MTAB-8658
NvElav1::mOrange+ transcriptome at 12dpf	ArrayExpress https://www.ebi.ac.uk/arrayexpress/	E-MTAB-8794
Nematostella vectensis genome	https://mycocosm.jgi.doe.gov/Nemve1/Nemve1.home.html	N/A
NvNCol3::mOrange2+ transcriptome	Sequence Read Archive at NCBI	PRJNA391807
Experimental Models: Organisms/Strains		
Nematostella vectensis	Sars Centre	N/A
Nematostella: NvElav1::mOrange	Sars Centre	N/A
Nematostella: NvNCol3::mOrange2	Yehu Moran lab	N/A
Nematostella: NvPOU4::memGFP	this study	N/A
Nematostella: *NvPOU4*$^{-/-}$	this study	N/A
Oligonucleotides		
Morpholino *NvSoxB2* MO1: TATACTCTCCGCTGTGTCGCTATGT	GeneTools	N/A
Generic control morpholino: CCATTGTGAAGTTAAACGATAGATC	Gene Tools	N/A
Oligonucleotide 1 for sgRNA *NvPOU4*: 5′TAGGCGTGGGTTCATATCATCGGC	Sigma	N/A
Oligonucleotide 2 for sgRNA *NvPOU4*: 5′AAACGCCGATGATATGAACCCACG	Sigma	N/A
Primer for melt curve analysis of *NvPOU4* mutants: forward: 5′CACGCGTTACACTCGGCAATCG	Sigma	N/A
Primer for melt curve analysis of *NvPOU4* mutants: reverse: 5′TCTTCTTTGCTTGAAGCGTTCCG	Sigma	N/A
Primer for sequencing of *NvPOU4* locus forward: 5′TCCCAAATACCTGACGAAACCAT	Sigma	N/A

(*Continued on next page*)

Continued		
REAGENT or RESOURCE	SOURCE	IDENTIFIER
Primer for sequencing of *NvPOU4* locus reverse: 5′CGTTTACGTTTCTTGTCGGAGTT	Sigma	N/A
Recombinant DNA		
Plasmid: *pNvPOU4::memGFP* (pUC57 backbone)	this study	N/A
Software and Algorithms		
Trimmomatic v0.38	http://www.usadellab.org/cms/?page=trimmomatic	N/A
STAR v2.7.0	https://github.com/alexdobin/STAR	N/A
Samtools v1.6	http://www.htslib.org	N/A
HTseq v0.11.2	https://htseq.readthedocs.io/en/release_0.11.1/	N/A
DESeq2 v1.26.0	https://bioconductor.org/packages/release/bioc/html/DESeq2.html	N/A
ClusterProfiler v1.13.0	https://bioconductor.org/packages/release/bioc/html/clusterProfiler.html	N/A
Imaris v8.4.1	Bitplane	N/A

LEAD CONTACT AND MATERIALS AVAILABILITY

Further information and requests for resources and reagents should be directed to and will be fulfilled by the Lead Contact, Fabian Rentzsch (fabian.rentzsch@uib.no). Plasmids and genetically modified *Nematostella vectensis* generated for this study are available upon completion of a Material Transfer Agreement.

EXPERIMENTAL MODEL AND SUBJECT DETAILS

Nematostella culture

The *Nematostella vectensis* culture is derived from CH2 males and CH6 females (Hand and Uhlinger, 1992). Adult polyps (> 12 months) were maintained at 18°C in 1/3 filtered seawater (= *Nematostella* medium, NM). Spawning induction was performed by light and temperature shift (18°C to 25°C) for 12 hours as described in Fritzenwanker and Technau (2002). Incubation of the fertilized egg packages with a 3% cysteine/NM for 20min removed the jelly. Embryos were then raised at 21°C and fixed at 12 hours post fertilization (hpf; early blastula), 16hpf (blastula), 20hpf (early gastrula), 24hpf (gastrula), 30hpf (late gastrula), 48hpf (early planula), 72hpf (planula), 4dpf (late planula); 5dpf (tentacle bud); 7dpf (early primary polyp), 12dpf (late primary polyp). The sex of the analyzed specimens was not determined. The high penetrance of phenotypes (100% for *NvPOU4* mutants) suggests that there are no significant differences between male and female animals in response to genetic manipulations.

Genetic crosses

The *NvSoxB(2)*::mOrange line has been described in Richards and Rentzsch (2014), *NvElav1*::mOrange in Nakanishi et al. (2012), *NvNCol3*::mOrange in Sunagar et al. (2018) and *NvFoxQ2d*::mOrange in Busengdal and Rentzsch (2017). *NvPOU4::memGFP*$^{+/-}$, *NvSoxB(2)* $^{+/-}$ double transgenics were generated by crossing *NvPOU4::memGFP*$^{+/-}$ to *NvSoxB(2)::mOrange* $^{+/+}$ animals; *NvPOU4::memGFP*$^{+/-}$,*NvElav1::mOrange*$^{+/-}$ double transgenics by crossing *NvPOU4::memGFP*$^{+/-}$ to *NvElav1::mOrange*$^{+/-}$ animals; *NvPOU4::memGFP*$^{+/-}$,*NvNCol3::mOrange2*$^{+/-}$ double transgenics by crossing *NvPOU4::memGFP*$^{+/-}$ to *NvNCol3::mOrange2*$^{+/-}$; *NvPOU4*$^{1/1}$ (= *NvPOU4*$^{-/-}$) mutants were derived from *NvPOU4*$^{1/+}$ x *NvPOU4*$^{1/+}$ crosses; *NvPOU4*$^{1/1}$, *NvElav1::mOrange*$^{+/-}$ animals were generated by crossing *NvPOU4*$^{1/+}$ to *NvPOU4*$^{1/+}$, *NvElav1::mOrange*$^{+/-}$ polyps; *NvPOU4*$^{1/1}$, *NvNCol3::mOrange2*$^{+/-}$ animals were generated by crossing *NvPOU4*$^{1/+}$ to *NvPOU4*$^{1/+}$, *NvNCol3::mOrange2*$^{+/-}$ polyps.

METHOD DETAILS

Cloning of *NvPOU4*, *in situ* hybridization, EdU labeling and immunohistochemistry

The *NvPOU4* sequence is derived from gene model Nve5471, retrieved from https://figshare.com/articles/Nematostella_vectensis_transcriptome_and_gene_models_v2_0/807696. Fluorescent and colorimetric *in situ* hybridizations and immunohistochemistry were performed as described in the Supplementary material in Richards and Rentzsch (2014): Embryos were fixed in 3.7%

formaldehyde/0.25% glutaraldehyde/NM for 2 min on ice, then in 3.7% formaldehyde/PTW (PBS+0.1%Tween20) for 1 h at 4°C. For colorimetric *in situ* hybridization, samples were rehydrated in PTW, and then incubated in 20 μg/ml Proteinase K for 10 min at room temperature (RT) followed by washes in 4mg/ml Glycine/PTW. They were then washed in 1% triethanolamine in PBS, followed by the addition of 0.25%, then 0.5% acetic anhydride. Samples were next washed in PTW and refixed in 3.7% formaldehyde/PTW, followed by washes in PTW. Pre-hybridization in hybridization buffer (HB: 50% formamide, 5X SSC, 1% SDS, 50 μg/ml heparin, 100 μg/ml salmon sperm DNA, 9.25 mM citric acid, 0.1X Tween20) was for at least 2 h at 60°C. Digoxigenin-labeled riboprobes were synthesized from PCR templates (MEGAscript Kit, Ambion) and incubated with the samples at a final concentration of 0.1-1 ng/μl for at least 60 h at 60°C. Unbound probe was removed via a series of 60°C washes of HB/2X SSC solutions [75/25, 50/50, 25/75, 0/100 (v/v)], then 0.2X SSC, 0.1XSSC. This was followed by RT washes of SSC/PTW solutions [75/25, 50/50, 25/75, 0/100 (v/v)]. Samples were then blocked in blocking solution [1% Block (Roche)/Maleic acid buffer (100mM maleic acid, 150mM NaCl)] for 2 h at RT and incubated overnight with 1:5000 anti-digoxigenin alkaline phosphatase (Roche)/blocking solution. Unbound antibody was removed with 10 × 15 min washes of PBTxBSA (PBS /0.2% Triton X-100 /0.1% bovine serum albumin); samples were then washed with staining buffer (100mM Tris pH 9.5, 100mM NaCl, 50mM MgCl2, 0.1%Tween20) before color was developed via the addition of 1:200 NBT/BCIP solution (Roche) in staining buffer. When the staining reaction was judged to be complete, samples were washed as follows – staining buffer, PTW, H20, ethanol, H20, PTW – and then post- fixed for 30 min with 3.7% formaldehyde/PTW before being washed with PTW and then cleared via overnight incubation in 87% glycerol at 4°C.

For fluorescent *in situ* hybridization, fixed samples were incubated in 2% hydrogen peroxide in methanol to quench endogenous hydrogen peroxidase activity. Samples were then rehydrated in PTW and the ISH protocol (see above) was followed from the Proteinase K incubation step until the end of the SSC/PTW RT washes. During hybridization, samples were incubated with either digoxigenin or fluorescein-labeled riboprobes (MEGAscript Kit, Ambion) at a final concentration of 1 ng/μl. After the SSC/PTW RT washes, samples were washed in TNT (0.1M Tris-HCl pH 7.5/0.15M NaCl/0.5% Triton X-100) and then blocked in TNTblock [0.5% blocking reagent (PerkinElmer)/TNT] for 1 h at RT before overnight incubation with anti-digoxigenin (1:100) or anti-fluorescein (1:250) horseradish peroxidase (Roche). Unbound antibodies were removed by 10 × 15 min TNT washes, and samples were then incubated in fluorophore tyramide amplification reagent (TSA Plus Kit, PerkinElmer). After the TSA reaction, samples were washed in TNT and then incubated with DAPI 1:1000 and mounted in ProLong Gold antifade reagent. For double labeling, samples were washed in 0.1M glycine pH 2.0 and then incubated 1 h in TNT block before overnight incubation with anti-digoxygenin or anti-fluorescein horseradish peroxidase (Roche). Post-antibody washing and the TSA reaction were repeated as for the first probe; samples were then washed in TNT, incubated with DAPI 1:1000 and mounted in ProLong Gold antifade reagent. Samples were imaged on either a Nikon Eclipse E800 compound microscope with a Nikon Digital Sight DSU3 camera or on a Leica SP5 confocal microscope.

For immunohistochemistry, fixed samples were washed for 2h with PBTx (PBS/0.3%Triton X-100) and then incubated in block (5% normal goat serum/PBTx) for 1h at RT before overnight incubation in primary antibodies at 4°C. Samples were then washed for 2h with PBTx, incubated for 1h at RT in block and then overnight at 4°C in Alexa Fluor conjugated secondary antibodies (Molecular Probes, 1:200). Samples were then washed for 2h with PBTx, incubated for 30 min in DAPI 1:1000 (Molecular Probes) and mounted in ProLong Gold antifade reagent (Molecular Probes).

The following primary antibodies were used: to detect *NvPOU4*::memGFP, anti-GFP (mouse, abcam1218, 1:200); to detect mOrange, anti dsRed (rabbit, Clontech 632496, 1:100); anti-NCol3 (Zenkert et al., 2011); mature cnidocytes were labeled with DAPI/EDTA as described in Babonis and Martindale (2017) and Szczepanek et al. (2002).

EdU labeling was done as described in Richards and Rentzsch (2014): Embryos were incubated with 100 μM EdU/DMSO in NM for 30 min at 21°C and fixed immediately afterward in 3.7% formaldehyde/0.25% glutaraldehyde/NM for 2 min on ice, followed by 3.7% formaldehyde/PTW (PBS+0.1%Tween20) for 1 h at 4°C. After the FISH protocol was completed, EdU incorporation was visualized using the Click-iT EdU Alexa Fluor 488 imaging kit (Molecular Probes C10337) following the manufacturer's instructions. For counting *NvPOU4*$^+$ and EdU$^+$ cells a 100 μm × 100 μm sampling area was defined in the mid-lateral region of the ectoderm at blastula stage. All the nuclei from this region were scanned via confocal microscopy.

Generation of transgenic lines

The *NvPOU4*::memGFP transgenic reporter line was generated by meganuclease-mediated transgenesis as described by Renfer and Technau (2017). The genomic coordinates for the 4.7 kb regulatory region are 1063816-1068603 on scaffold 16 (http://genome.jgi.doe.gov/Nemve1/Nemve1.home.html, accessed 15 April 2019). This fragment was inserted in front of a codon optimized GFP via the HiFi DNA Assembly kit (NEB) with the addition of a membrane-tethering CAAX domain at the C terminus to visualize the morphology of the cells expressing the reporter protein. The reporter cassette is flanked by inverted I-SceI sites, the vector backbone is pUC57. memGFP was detected with an anti-GFP antibody (mouse, abcam1218, 1:200).

CRISPR-Cas9 mediated mutagenesis and genotyping of embryos

Using published methods (Ikmi et al., 2014; Kraus et al., 2016) sgRNA were synthesized *in vitro* via the Megashortscript T7 kit (Invitrogen) using the following oligos: 5′TAGGCGTGGGTTCATATCATCGGC, 5′AAACGCCGATGATATGAACCCACG

The reaction mixture (500 ng/μl Cas9 enzyme [PNA Bio CP01] and 150 ng/μl of the sgRNA) was incubated at 37°C for 15min prior to injection.

Genomic DNA from embryos or aboral pieces of F1 polyps was extracted using a Tris/EDTA/proteinase K buffer. Mutant genotyping was first done via melt-curve analysis after PCR amplification of a 90bp region on a BioRad CFX96 RealRime PCR machine. Mutations were confirmed by sequencing a 500bp region around the mutation.

Primers for melt curve analysis are: 5′CACGCGTTACACTCGGCAATCG (forward) and 5′TCTTCTTTGCTTGAAGCGTTCCG (reverse). Primers for sequencing are: 5′TCCCAAATACCTGACGAAACCAT (forward) and 5′CGTTTACGTTTCTTGTCGGA GTT (reverse).

Morpholino injection

NvSoxB(2) MO1 is described in Richards and Rentzsch (2014), the sequence is TATACTCTCCGCTGTGTCGCTATGT. The sequence of the generic control morpholino is CCATTGTGAAGTTAAACGATAGATC. Fertilized eggs were injected with 500 μM morpholino (Gene Tools) and 40 μg/ml Alexa Fluor-conjugated dextran (Invitrogen) diluted in water. The injections were performed using a Femtojet microinjector (Eppendorf) and a Nikon TE2000-S inverted microscope. Experiments were conducted with four biological replicates, with embryos derived from four independent spawnings.

Generation of transcriptomes from *NvPOU4* mutants and siblings

The presence/absence of cnidocysts was used for sorting animals at primary polyp stage (12dpf) into sibling control (*NvPOU4*$^{+/+}$ and *NvPOU4*$^{+/-}$) and mutants (*NvPOU4*$^{-/-}$). Twenty primary polyps were pooled for each biological condition and the total RNA was extracted using the Direct-zol RNA MicroPrep kit (Zymo Research). Experiments were conducted with four biological replicates, with embryos derived from four independent spawnings. Sequencing libraries were generated with the TruSeq® stranded mRNA library prep kit (Illumina), 75bp single read sequencing was performed on a NextSeq500 machine (Illumina).

Cell type specific transcriptomes

NvElav1::mOrange-positive cells were enriched by FACS and RNA was extracted as described previously (Torres-Méndez et al., 2019): mOrange positive primary polyps (12-14 days old) were dissociated at 37°C for ~30 min in calcium- and magnesium-free *Nematostella* medium (CMF/NM) containing EDTA and 0.25% of trypsin. Single cell suspensions were then stained at room temperature with Hoechst 33342 and 7-aminoactinomycin D (7-AAD) to exclude debris and non-viable cells by Fluorescent-Activated Cell Sorting (FACS). Sorting was performed on a BD FACSAria II Sorp. with 100μm nozzle.

cDNA was prepared from 400pg of total RNA using the Smart-Seq 2 method with 16 pre-amplification PCR cycles, as described by Picelli et al. (2014). NGS libraries were prepared using the home-made tagmentation-based method as described by Hennig et al. (2018). Briefly, 125ng of cDNA was tagmented using home-made Tn5 loaded with annealed linker oligonucleotides for 3 minutes at 55°C. Reactions were inactivated by adding 1.25μl of 0.2% SDS and incubation for 5 minutes at room temperature. Indexing and amplification was done using the KAPA HiFi HotStart PCR kit (Sigma-Aldrich) with Index oligonucleotides (sequences were adapted from Illumina). Four biological replicates of mOrange-positive and -negative cells, respectively, were used for 75bp single read sequencing on a NextSeq500 machine (Illumina).

The generation of *NvNCol3*::mOrange2 transcriptomes is described in Sunagar et al. (2018). In brief, tentacles of transgenic *Nematostella* polyps were dissociated and sorted in a FACSAria III (BD Biosciences, USA). Total RNA was isolated using TRIZOL LS, libraries were prepared by the Illumina TruSeq RNA library protocol (mean insert size of 150 bp) and sequenced on Illumina Nextseq 500 high output v2 platform.

QUANTIFICATION AND STATISTICAL ANALYSIS

Transcriptome analyses

The raw fastq files were initially quality checked and trimmed using Trimmomatic v0.38 (Bolger et al., 2014). Following this they were aligned to the *N. vectensis* genome (https://mycocosm.jgi.doe.gov/Nemve1/Nemve1.home.html) using STAR v2.7.0 (Dobin et al., 2013) in two-pass mode. Afterward the produced BAM (Binary Alignment Maps) files were sorted and indexed with Samtools v1.6 (Li et al., 2009) and then gene counting was carried out using HTSeq v0.11.2 (Anders et al., 2015). Gene models were retrieved from (https://figshare.com/articles/Nematostella_vectensis_transcriptome_and_gene_models_v2_0/807696). Differential gene expression testing and subsequent over-representation analysis was done in R with DESeq2 v1.26.0 (Love et al., 2014) and clusterProfiler v1.13.0 (Yu et al., 2012), respectively.

Quantification of *NvPOU4* expression upon *NvSoxB(2)* MO injection

The frequencies of the phenotypic categories (wt, weak, none) are shown as mean ± SD (four biological replicates). Significance was tested by chi-square test for control MO versus *NvSoxB(2)* MO for the three different categories using the count data from the four biological replicates.

Quantification of *NvElav1*::mOrange^{+} cells in *NvPOU4* mutants and siblings

NvElav1::mOrange positive cells (stained with anti dsRed antibody) were counted in an area 100μm long and located between two mesenteries. The quantification was done in animals from four different spawnings and with 5-10 animals per sample. The genotype

was inferred *a posteriori* by the presence/absence of cnidocysts. A Shapiro-Wilk test was used to determine whether the data follow a normal distribution. t test was performed for normal distribution, Mann Whitney test (U-test) was performed for abnormal distribution. Differences were considered not significant when $p > 0.05$. Box and whisker plots were generated with the default settings of Excel, quartiles were calculated using Exclusive median. Boxes indicate first and third quartile, whiskers indicate 1.5 x interquartile range, outliers are shown as dots.

DATA AND CODE AVAILABILITY

The accession number for the source transcriptome data for *NvPOU4* mutants and siblings reported in this study is ArrayExpress: E-MTAB-8658. The accession number for the source transcriptome data for *NvElav1*::mOrange-positive and –negative cells, respectively, is ArrayExpress: E-MTAB-8794. No new code was generated for the study.